An Advanced Conceptual Tokamak Fusion Power Reactor Utilizing Closed Cycle Helium Gas Turbines

R.W. Conn and S.C. Kuo

March 1976

UWFDM-156

FUSION TECHNOLOGY INSTITUTE

UNIVERSITY OF WISCONSIN

MADISON WISCONSIN

An Advanced Conceptual Tokamak Fusion Power Reactor Utilizing Closed Cycle Helium Gas Turbines

R.W. Conn and S.C. Kuo

Fusion Technology Institute
University of Wisconsin
1500 Engineering Drive
Madison, WI 53706

http://fti.neep.wisc.edu

March 1976

UWFDM-156

An Advanced Conceptual Tokamak Fusion Power Reactor
Utilizing Closed Cycle Helium Gas Turbines

Robert W. Conn

Fusion Technology Program
Nuclear Engineering Department
University of Wisconsin
Madison, Wisconsin   53706

and

Simion C. Kuo

United Technologies Research Center
East Hartford, Conn.   06108

March 1976

Abstract

UWMAK-III is a conceptual tokamak reactor designed to study the potential and the problems associated with an advanced version of tokamaks as power reactors. Design choices have been made which represent reasonable extrapolations of present technology. The major features are the noncircular plasma cross section, the use of TZM, a molybdenum based alloy, as the primary structural material, and the incorporation of a closed cycle helium gas turbine power conversion system. The blanket design is unique in that tritium breeding is accomplished in the liquid lithium coolant of the outer blanket only. The inner blanket zone nearest the torus centerline is a hot shield cooled with helium. The reactor is designed to generate 4735 MW_t and 1985 MW_e continuously. The reference design for the power conversion system was selected based on trade-off considerations and an examination of interface problems. Three loops with turbomachinery rated at 585 MW_e have been incorporated and the helium inlet temperature is 1600°F (871°C). A conceptual design of the turbomachinery is given together with a preliminary heat exchanger analysis that results in relatively compact designs for the regenerator, precooler, and intercooler. The paper contains a general description of the UWMAK-III system and a discussion of those aspects of the reactor, such as the burn cycle, the blanket design, and the heat transfer analysis, which are required to form the basis for discussing the power conversion system. We concentrate on the power conversion system and include a parametric performance analysis, an interface and trade off study and a description of the reference conceptual design of the closed cycle helium gas turbine power conversion system.

1. Introduction

The UWMAK-III conceptual tokamak reactor study has had as its principal goal the detailed self-consistent examination of an advanced tokamak fusion power reactor. The UWMAK-II study described in another paper of this journal[1] differed in that design choices were based wherever possible on present day technology with the major example the choice of 316 stainless steel as the primary structural material. For UWMAK-III, a number of design choices are made which represent reasonable extrapolations of present technology in the context of the general time frame envisioned for widespread practical application of controlled fusion. The prime examples are the choice of the molybdenum based alloy, TZM (99.4% Mo, .08% Zr, .5% Ti, 0.01%C) as the structural material and the use of aluminum as the stabilizer and structure in the toroidal field magnets. On the other hand, many of the design features are generic and therefore applicable to near term tokamaks as well. Examples here include the unique blanket design, the MHD analysis and the plasma shape, the method of particle collection in the divertor, the use of RF heating to bring the plasma to ignition conditions, the tritium extraction and recycling processes, and the general design approach to module removal.

The purpose of this paper is to give a general description of the UWMAK-III conceptual reactor system and to concentrate on details related directly to the power conversion system. As such, after the overall description given in section 2, a discussion of the plasma burn cycle for tokamaks generally and for UWMAK-III in particular is given in section 3. The particle divertor system and its associated power cycle is described in section 4 while the design and neutronics performance of the blanket system is given in section 5. The burn cycle and the blanket design analysis provide the basic input to the discussion of the closed cycle gas turbine power conversion system. We discuss first the power conversion system requirements and

constraints in section 6 and then describe a parametric analysis and trade-off study related to the selection of the operating conditions and economics of the power system in sections 7 and 8. Based upon the results presented in these sections, a description of the conceptual closed cycle helium gas turbine power conversion system developed for UWMAK-III is given in section 9. Conclusions are given in section 10.

2. General Description of the UWMAK-III Conceptual Tokamak Reactor System

An overall view of the UWMAK-III reactor is shown in Fig. 1 and a detailed cross section view of the nuclear island is given on Fig. 2. A summary of the major parameters and characteristics of the design is given in Table 1. A complete report on all details of this reactor study is given in ref. 2. The reactor is designed to generate 5000 MW_t during the deuterium-tritium plasma burn and 4735 MW_t continuously. The net electrical output is 1985 MW_e. The design has a number of unique features, one of which is the noncircular plasma shape produced by discrete coils outside the blanket and shield zones. The plasma is bounded by a separatrix with two null points in the poloidal magnetic field symmetrically located above and below the horizontal midplane that provides for a poloidal divertor.

The reasons for choosing a noncircular cross section are to take advantage of the potential for higher total beta (the ratio of plasma to magnetic field pressure) and therefore to increase the power density in the plasma without substantially increasing the toroidal magnetic field.[3] The scaling is

$$\beta = \beta_\theta \left(\frac{S}{qA}\right)^2$$

where β_θ is the poloidal beta, A is the aspect ratio of the plasma and q is the plasma safety factor. S is the shape factor and is equal to the ratio of the circumference of the plasma cross section divided by the circumference of the inscribed circle. A circular plasma has S equal to 1. For UWMAK-III, A is 3

Table 1

MAJOR CHARACTERISTICS AND PARAMETERS OF UWMAK-III

Structural Material	Mo Alloy, TZM
Coolant	
Inner Blanket	He
Outer Blanket	Lithium
Fuel Cycle	(D-T), Li
Number of Toroidal Field Magnets	18
Magnet Superconductor	NbTi
Magnet Structural Material	Al Alloy
Maximum Magnetic Field	8.75T
On Axis Magnetic Field	4.05T
Plasma Dimensions	
Major Radius	8.1m
Half Width	2.7m
Height to Width Ratio	2
Plasma Shape	"Triangular D"
Plasma Current	15.8 MA
Impurity Control Method	Divertor + Low Z Liner
Plasma Heating Method	RF (Fast Wave – 60 MHz)
Burn Time	1800 sec
Duty Factor	0.947
Breeding Ratio	(1.074-1.3)
Average Neutron Wall Loading	1.91 MW/m^2
Power Cycle	
Blanket	Closed Cycle He
Divertor	Na-Steam
Power Output During Burn	5000 MW(th)
Average Electrical Output	1985 MW$_e$
Net Plant Efficiency	41.9%

and S is 1.6. Of course, the potential benefits of noncircular tokamaks will only be realized if a plasma can be kept in equilibrium at values of q and β_θ similar to those in circular cross section plasmas. If, for example, q must be increased to maintain plasma stability in noncircular systems, the desired increase in β will not come about.

Therefore, a detailed MHD equilibrium and stability study has been carried out to determine the proper plasma shape.[4] A list of the characteristic parameters that go along with this plasma design is given in Table 2. The main parameters are the plasma current, 15.8 MA; the axial magnetic field, 4.05 T; the major radius, 8.1 m; plasma shape factor, 1.6; plasma width at the midplane, 5.4 m; average poloidal beta, 2.2; aspect ratio, 3; and stability factor, q(o), on axis, ~1. The plasma has been satisfactorily tested for stability against rigid displacements, general kink modes, and localized interchange modes. The large triangularity of the plasma shape is the result of forcing the vacuum vertical field to have good curvature in the region to the right of the magnetic axis at R_m = 9.0 m. The stability factor near the separatrix is above 3. This appears reasonable for future machines.

A second major characteristic of UWMAK-III is its substantially reduced size compared with our earlier studies, UWMAK-I[5] and UWMAK-II[1,6] which have the same thermal power output during the plasma burn. The previous designs had circular plasmas with a major radius of 13 m compared with 8.1 m in the present study. A comparison of the plasma shape and the toroidal field magnet size for UWMAK-II and UWMAK-III is shown in Fig. 3. The size reduction is made possible by the design decision to increase the 14 MeV neutron wall loading from ~1 MW/m^2 previously to approximately 2 MW/m^2 in UWMAK-III and by the higher value of power density in the noncircular plasma. The higher value of neutron wall loading was in turn made possible by the unique blanket design based on the concept of using graphite as a neutron spectrum shaper to protect the first structural wall from radiation damage.[7,8] This will be discussed shortly.

Table 2

Plasma Characteristics of UWMAK-III

Major Radius	8.1 m
Plasma Half Width	2.7 m
Plasma Height to Width Ratio	~2
Plasma Current	15.8 MA
Plasma Shape Factor	1.6
On Axis Toroidal Magnetic Field	4.05 T
Maximum Toroidal Field at Coil	8.75 T
Average Poloidal Beta, β_θ	2.2
Average Total Beta, β	0.09
Stability Factor on Axis	~1
Stability Factor Near Separatrix	~3.5

Another unusual feature in this work is the magnet design, which uses NbTi superconductor with Al as the stabilizer and a high strength Al alloy as the magnet structural material.[9] The use of high purity Al as the stabilizer allows one to reduce the amount of stabilizer by a factor of 2 to 5 compared with the use of Cu. Alternatively, because the resistance of Al is lower than for Cu, the heat generated due to I^2R losses is less when the same amount of material is used. All this makes for a better stabilizer. In addition, experiments at the University of Wisconsin have shown that when reinforced, as it is in a magnet, high purity Al does not develop a high resistivity when stressed beyond its yield point.[10] The use of an Al alloy provides a structure of almost equal strength to the use of 316 stainless steel at about one third the weight. It also means there will be a compatible contraction of both the conductor and the structure on cool down.

The blanket and shield design is unique and can be most readily understood by examining the schematic illustrated in Fig. 4. The inner blanket and shield closest to the torus centerline is not designed to breed tritium but only to extract heat and protect the superconducting toroidal field magnets. As such, it really constitutes a shield which is divided into hot and cold zones. Greater than 99% of the energy incident on the inner shield is deposited in the hot zone composed of structure (TZM), boron carbide (B_4C), and helium coolant. The cold inner shield uses 316 stainless steel as the structure. In front of the first wall of the inner shield is a 25 cm graphite zone which is passive (not actively cooled) and which serves to soften the neutron spectrum incident on the first structural wall.[7] This in turn reduces the radiation damage to the structure and the inner hot shield is designed for plant life. This passive graphite is referred to as an internal spectral shifter and energy convertor, or ISSEC.

The outer blanket is cooled with liquid lithium which also acts as the breeding material. The overall breeding ratio ranges from 1.074 to 1.27 depending on the calculational method but nonetheless exceeds 1. Very detailed recent calculations in toroidal geometry give a breeding ratio of 1.25.[11] The structural material in the outer blanket is not protected from 14 MeV neutrons and therefore will have to be replaced periodically because of radiation damage. The wall life is estimated to be about 2 years. However, the outer portion of

a torus is where space is plentiful so that the difficulties involved in blanket module replacement are at least minimized.

The use of a refractory metal alloy as the structural material was primarily motivated by the desire to increase the operating temperature of the coolant to increase the overall efficiency of the power cycle. The choice of the molybdenum based alloy, TZM, over alloys of vanadium or niobium was based on the good high temperature creep strength and fatigue life of TZM, its compatibility with both helium and liquid lithium, its low permeation to tritium, its good neutronics properties, its relatively low cost and the good resource position of the United States with respect to Mo. The problem associated with joining TZM is recognized and has been examined elsewhere.[12]

A final feature of the UWMAK-III design is the use of a helium power cycle which we shall concentrate on in this paper. The coolant from the inner blanket goes directly to a helium turbine while the lithium from the outer blanket goes to an intermediate, Li-Na heat exchanger, and the sodium subsequently goes to a Na-He heat exchanger from which the He is used to drive the turbines. Sodium from the intermediate loop plays the dual role of isolating the tritium containing lithium from the power cycle and providing a working fluid for thermal energy storage which can be used during the down part of a Tokamak plasma cycle to keep a continuous hot helium flow to the turbines.

The power conversion system therefore has two distinct components, the power cycle associated with the heat deposited in both the inner hot shield and the outer blanket, and the heat deposited in the divertor by particles diffusing from the plasma. The advanced power conversion system designed for the high temperature coolants of the inner hot shield and the outer blanket is based on a closed-cycle helium gas turbine system and yields a total power output of

1755 MWe. The divertor power cycle associated with the heat transport from the plasma in the form of hot particles is based on a conventional Rankine steam power cycle to utilize the 687 MW_t (average) in the divertor. The sodium coolant of the divertor plates leaves the reactor at 600°C and the total power output is 295 MW_e. The calculated gross electrical power output is 2050 MW_e and the net electrical output is 1985 MW. This gives a net plant efficiency of 41.9%.

3. Tokamak Plasma Burn Cycle

A tokamak is inherently a pulsed plasma device because it is based upon the plasma acting as a single turn secondary of a transformer. Since there is a limit to the ability of the transformer to induce current flow in the secondary, the current induced to flow in the plasma must be turned off, the primary windings reset, and the cycle started again. There have been theoretical predictions that a bootstrap current associated with the diffusion process should exist in hot tokamaks.[13] If so, this would allow current to flow in the plasma without requiring transformer action and would thus allow truly steady state operation. However, this prediction has not been verified experimentally even under circumstances where it should have been measurable. As such, we assume here that the bootstrap current does not exist and that the tokamak plasma burn is limited.

There are four distinct phases to the tokamak reactor burn cycle: startup, auxiliary plasma heating to ignition and burn conditions, plasma burn at steady thermonuclear conditions, and finally plasma shutdown and preparation for restart. Startup is the phase when the D-T gas in the vacuum chamber breaks down and the plasma current is raised to the desired operating value. The plasma is ohmically heated during this time and reaches a temperature of 1-3 keV. We

have not considered auxiliary heating to raise the plasma temperature further during startup although this may be both possible and advantageous.

Optimum thermonuclear burn conditions in D-T occur when the ion temperature is about 15 keV. It is therefore necessary to provide for auxiliary plasma heating during a second phase of the burn cycle. As the ion temperature is raised, it passes through an ignition point above which the plasma is further heated spontaneously by alpha particles until a steady state condition is reached. Assuming the plasma density is now maintained by external fueling with cold D-T, the plasma burns and produces the energy that is converted to electricity.

The plasma burn time in tokamaks may be limited by several things but theoretically, the burn could be quite long. One limiting factor is magnetic flux in the core of the transformer and the maximum current which the primary windings can carry. If this is so, the burn could readily be thousands of seconds. Another unrelated limiting factor is the influx of impurities from the vacuum chamber walls. Plasma particles diffuse out of the main confinement region and if they end up striking the vacuum chamber, they can give rise to sputtering, desorption, and other phenomena that produce impurities which can find their way into the plasma. The effects of impurities have been reviewed elsewhere[14] but suffice it to say their effect is detrimental. It leads to excessive energy loss from the plasma and can cause it to become unignited. In UWMAK-III, two forms of impurity control have been incorporated, a low Z liner (carbon) and a divertor. We discuss the divertor concept shortly but for the present discussion, it is assumed that long burn times are possible.

At the end of the burn, the plasma current is reduced to zero, the chamber is pumped of residual gas, fresh D-T gas is admitted, and the cycle starts again.

The cycle designed for UWMAK-III is summarized in Table 3. The important point for the power cycle is that the plasma produces energy essentially only during the burn phase. Yet it is necessary to produce electricity continuously and this leads to the requirement for some form of energy storage. Thermal storage is used in UWMAK-III and details are discussed in sections 6-9.

4. Divertor Operation and Associated Power Cycle

The fusion of deuterium and tritium releases 17.6 MeV of energy in the form of a 14.1 MeV neutron and a 3.5 MeV alpha particle. The neutron escapes from the plasma region and is slowed down and captured in the surrounding blanket region. The alpha particle, however, is trapped by the confining magnetic field and slows down against the background D-T plasma. In the process, it heats the plasma and in steady state this fusion energy input balances plasma energy losses due to particle leakage, conduction, and radiation. Radiation from the plasma as well as cross field conduction constitutes a surface energy load on the vacuum chamber wall which is converted to electricity via the power cycle associated with the blanket system. The energy in charged particles diffusing from the plasma will also reach the first wall if no other steps are taken.

For several reasons, it may be critically important to prevent excessive bombardment of the first wall by energetic particles. In the first place, such bombardment would give rise to sputtering and desorption which in turn leads to a gas and impurity influx to the plasma. The impurity influx is particularly troublesome since it can lead to excessive radiative losses and cause the plasma

Table   3

UWMAK - III REACTOR CYCLE

Time(Sec).	Phase
0-15	Startup: Plasma and divertor currents rise to full value; transformer currents begin to drop.
15-30	RF Heating: Plasma and divertor currents at full value; transformer currents continue to drop.
30-1830	Burn: Transformer currents drop to maximum negative value.
1830-1850	Shutdown: Plasma and divertor currents drop to zero; transformer currents rise to provide negative startup flux.
1850-1890	Pumpout and recharge: First 20 seconds, hydrogen gas pumped in to cool plasma, residual gas pumped out. Final 20 seconds; transformer currents reset to initial values.
1890-1900	Final pumpout and refill: Chamber purged and refilled with fresh fuel.

temperature to drop sharply. This would cause the plasma to shut down and require a pumpout and restart of the burn cycle. In particular, excessive impurity influx can limit the allowable burn time and thus make it difficult to achieve a good duty factor. Secondly, bombardment by energetic particles will cause wall erosion and a thinning of the first wall with time.

For these reasons, a poloidal magnetic divertor has been designed for UWMAK-III and the cross section view shown in Fig. 5 illustrates this system most clearly. The plasma is bounded by a separatrix and has two null points in the poloidal magnetic field located symmetrically above and below the plasma midplane. Particles on field lines inside the separatrix remain confined to this interior region. However, particles which once diffuse across the separatrix are now on field lines that carry them above or below the main confinement region. Particle collector plates as shown in Fig. 4 are strategically located to stop these particles and to collect their energy. In the process, the particles diverted to the collector plates are prevented from striking the first wall.

The main point for the purposes of this paper is that the power associated with these particles can be as much as 10-20% of the thermal power output of the system. The exact amount will ultimately depend on the nature of the plasma physics but for UWMAK-III, we have estimated that 725 MW_t of the 5000 MW_t total is carried by particles to the collector plates during the plasma burn. This is equal to 687 MW_t averaged over one burn cycle. It is therefore important to collect this heat at high temperature and to convert it to electricity.

The design of the divertor in UWMAK-III is unique in several ways. Firstly, the particles bombard a thin, solid plate of TZM located <u>outside</u> the toroidal field magnets and the pumping and heat transfer problems are not coupled. Placing

the bombardment plates outside the TF coils allows the field lines to be fanned out, thus reducing the power density of particles on the plates. Combining this with the relatively small flow conductance back through the slots to the plasma, we expect that there will be little backstreaming of neutrals and impurities.

The particles get from the plasma to the collectors by following magnetic field lines into the fringing region of the toroidal field coils. These field lines get "caught" in the poloidal component of the fringing toroidal field and pass through the gaps between the coils.

The location of the particle collector plates is also shown in Fig. 5. This is based on the assumption that the coils are protected by the magnetic field against bombardment. This arrangement requires two collectors back-to-back to receive the flux from the inner and outer scrape-off zones. The particles from the inner scrape-off zone pass by the supports for the portion of the blanket and shield directly above and below the plasma. These supports are guarded against charged particle bombardment by two parallel currents. The line currents create a separatrix and thereby divert the field around the supports. The required current to guard the supports is 1.9 MA per support. Because of the location behind the blanket and shield, this can be a supercon-ducting current.

The particle collection plates in UWMAK-I[5] and II[6] consisted of a flowing lithium film to absorb both the D,T particles and the associated thermal energy. This design is not suitable for UWMAK-III due to the very large thermal

load carried on the plates. The average thermal load in UWMAK-I was 1.0 MW/m^2. This load increased to 3 MW/m^2 in UWMAK-II, with the peak load estimated to be around 30 MW/m^2. The lithium temperature can only vary from 186°C (its M.P.) to 350°C (the B.P. at the plasma chamber pressure 10^{-5} torr). With this very small coolant temperature rise available, and with the intense thermal load, the heat transfer problem becomes almost insurmountable.

The main structure of the collector plate will consist of a bank of tubes which form the coolant passages.[15] To avoid excessive sputtering due to incident high energy particles, a thin sheet of TZM is used to cover the main plate. Good thermal contact between the sheet and the plate is maintained by means of a liquid lithium film which fills the void between them. The main sheet of TZM acts as a sacrificial wall and is designed to allow frequent replacement. Two schematic drawings of the particle collector plate are shown in Fig. 6 and 7. There are 36 collector plates, each 1.14 m wide and 3 m high, giving a total surface area of 123 m^2. The sacrificial wall is 0.1 mm thick, weighing a total of 125 kg per exposed section.

Since the sacrificial wall has to be replaced frequently, a periodic automatic replacement process is envisaged which is shown schematically on Fig. 6. The thin TZM sheet is fed from a supply roller and taken up on a spent roller. A frozen lithium seal is provided on the periphery of the plate to prevent lithium from leaking out. After a TZM sheet has been in service for 17 hours, the peripheral seal is melted and the sheet advanced until new material covers the plate. The seal is then allowed to solidify again. This process can be carried out during a burn cycle with no downtime for the reactor.

The TZM plate is cooled with sodium and a calculation of the MHD effects on pressure drop from both Hartmann and end-of-loop effects has been made. The total pressure drop is 100 psi and the sodium exit temperature is 600°C. This sodium is then used to feed a conventional Rankine steam power cycle. The steam conditions are 2400 psig at 1000°F reheat. The sodium returns at 400°C and the net output from this cycle is 295 MWe. This is a substantial improvement over previous designs[5,6] in which the use of liquid lithium to collect the particles limited the lithium outlet temperature to only 325°C. This limited the efficiency of the divertor cycle to only 25%. As such, the design here is much more compatible with the overall high performance of UWMAK-III.

5. Blanket Design and Neutronics Analysis

The philosophy behind the blanket design in UWMAK-III was described in the introduction and a schematic illustration of the overall design is given in Fig.4. The neutronics behavior of this design was analysed using one and two dimensional S_n calculations with 46 neutron groups and 21 gamma groups.[5,6] In addition the source was described as a sharply peaked function near the magnetic axis and the shift of the magnetic axis from the geometric center due to finite β effects has been included.

Two dimensional calculations based on x-y geometry for a vertical cut through the torus were performed using the model shown in Fig. 8 . The major results are listed in Table 4 which shows a breeding ratio of 1.074 and an energy per fusion of 21.7 MeV. (More recent calculations in toroidal geometry show the breeding ratio of this design actually exceeds 1.2 without breeding in the inner blanket.[11]) Importantly, we also show the displacements per atom (dpa) rate and the helium production rate in the first structural wall on the inside of the torus behind the 25 cm graphite zone and in the first structural wall of the outer blanket. One can see that the dpa rate in the inner structural first wall is smaller by a factor of 6 and the helium production rate is smaller by a factor of 15 compared with the rates in the outer blanket first wall. Based on radiation damage consideration, we therefore expect the inner blanket to have a much longer life than the outer blanket.

Table 4

Nuclear Performance of UWMAK-III Blanket Design

Breeding Ratio	1.074
Energy per Fusion	21.7 MeV
Energy Attenuation	
of Inner Blanket and Shield	3×10^{-7} MeV/MeV
of Outer Blanket and Shield	3×10^{-7} MeV/MeV
Power in Blankets	4002
Power in Shields	47
DPA Rate Per Year	
Inner Blanket First Wall	2.9
Outer Blanket First Wall	18.8
Helium Production Rate (Appm/Yr)	
Inner Blanket First Wall	10.8
Outer Blanket First Wall	157.0
Average 14 MeV Neutron Wall Loading (MW/m^2)	1.91

The blanket design described in section 2 has three distinct components from a heat transfer viewpoint; the hot inner shield, the partial ISSEC of 25 cm graphite, and the outer breeding blanket. The neutronics calculations give the local neutron and gamma heating rates required as input to the heat transfer analysis. The heat transfer analysis and mechanical design have been carried out by D. K. Sze and I. Sviatoslavsky.[16]

The maximum allowable temperature in the graphite is yet to be defined. This temperature limitation may be set by any one of the following processes:

1. Evaporation, causing the carbon vapor to be condensed on the cryogenic pump panels.

2. Evaporation, causing impurity buildup in the plasma.

3. High temperature inside the ISSEC, causing carbon transport within this zone.

4. Formation of hydrocarbons, particularly acetylene, at temperatures approaching 1800-2000 C.

In this study, it is assumed that the maximum allowable temperature is 2000 C.

The heat deposited in the partial ISSEC zone will be transported to the front and back surfaces and radiated away. Thus, the maximum temperature will occur inside the graphite rather than at its surface. The heat transfer calculations show the temperatures in the ISSEC are within the specified limits if the graphite has a thermal conductivity comparable with 890S graphite, i.e., the surface temperature is $\leq$ 2000 C and the maximum temperature in the interior is ~2300 C. The recent toroidal geometry neutronics calculations referred to earlier [11] show that the heat deposition is reduced by about 25% compared with the x-y analysis. As such, the temperatures within the graphite will drop accordingly and nuclear grade graphite could be used without exceeding the specified temperature limits.

The thermal energy in the ISSEC will be radiated away and this leads

to high surface heating loads on the first structural walls. These are

calculated to be 35 W/cm^2 on the TZM first wall of the inner hot shield and

25 W/cm^2 on the outer first structural wall.

Two of the most severe problems in the design of a lithium cooled outer

blanket are MHD problems and thermal recirculation problems. The MHD problems

are caused by the circulation of electrically conducting lithium across

magnetic field lines. The thermal recirculation problems are caused by the

proximity of hot and cold lithium streams. The major feature of the outer

blanket design in UWMAK-III is to minimize these two effects.

The basic shape of a heat transfer unit is U-shaped as

in UWMAK-I [5]. This heat transfer cell design gives the lowest possible $\underline{V} \times \underline{B}$

value within the blanket and therefore minimizes MHD effects. However,

this shape has to be modified to prevent heat transfer between adjacent legs

of the cell. Fig. 9 shows a heat transfer cell for the UWMAK-III blanket.

The width of the cell is 37 cm, which is feasible because of the very low pressure

within the blanket. There is a 10 cm wide static lithium zone in the middle of the

cell which serves as thermal insulation despite the high thermal conductivity

of the lithium. The reason is that most of the heat is generated within the lithium

itself. The important dimensions of the outer blanket are given in Table 5.

The lithium coolant pressure drop has been calculated using the local

magnetic field, B, consisting of poloidal and toroidal components. The maximum

TABLE   5

Important Dimensions of the Outer Blanket

Thickness of the First Wall	1.5 mm
Width of the U-Cell	37 cm
Width of the Lithium Gap	10 cm
U-Cell Wall Thickness	6 mm
Baffle Wall Thickness	2 mm
First Breeding Zone Thickness	60 cm
Refractory Zone Thickness	30 cm
Second Breeding Zone Thickness	10 cm
Percentage Structure in the Blanket	3%
Diameter of the Header	20 cm
Wall Thickness of the Header	2 mm
Diameter of the Feed Tube	50 cm
Wall Thickness of the Header	5 mm

coolant pressure on the first wall is only 70 psia and the pumping power required is just 2 MW. These low values are possible because lithium is used only to cool the outer blanket where the magnetic field is low and where good access reduces losses in the headers and feed pipe systems. A two dimensional finite difference method has been used to calculate the temperature profile for a typical cell and the results are given in Fig. 10. The maximum temperature of the TZM structure is 1000 C and the exit temperature of the lithium to the power conversion system is 980 C.

The inner hot shield, or inner blanket, in UWMAK-III is cooled with helium. A 0.5m diameter feed tube is introduced between the toroidal field magnets and connected to a manifold running in the toroidal direction (see Fig. 2). The surface heat load on the inner blanket is 35 W/cm^2 and, together with the space dependent volumetric heating from the neutronics analysis, leads to a coolant inlet temperature of 488 C and an outlet temperature of 870 C at 1000 psi pressure. These coolant conditions match the temperature of the helium coming from the secondary heat exchanger of the outer blanket cycle such that identical turbines and thermal energy storage can be used. This is discussed in sections 6-9.

The distribution of coolant tubes within the inner blanket is arranged to be inversely proportional to the heating rate so that the heat load on each coolant tube is approximately the same. The design is shown in Fig. 11. Large amounts of Mo are used in the inner blanket for shielding reasons, most of which can be in the less expensive form of powder. However, because both powdered Mo and B_4C are poor thermal conductors, we find that approximately 35% of the total Mo has to be in the form of fine sheet that is oriented to provide a conduction path to the TZM coolant tubes. The maximum allowable temperature in the B_4C and nonstructural Mo is assumed to be 1250 C.

The total amount of power deposited in the inner and outer blanket zones is important input to the power conversion system study. Based on the x-y neutronics calculations, we find 1334 MW_t is produced in the inner blanket while 2668 MW_t is produced in the outer blanket. These values are averaged over one burn cycle and, when added to the average of 687 MW_t from the divertor system, give 4735 MW_t continuous as the thermal power rating for UWMAK-III.

6. Power Conversion System Requirements and Constraints

The choice of a particular power conversion system for a fusion power plant depends to a large extent on such factors as the choice of blanket coolant, the temperature capability of the blanket, the energy storage scheme used, the operating temperature and efficiency of the heat engine, the specified power rating, and, most important of all, the capital cost of the entire power station ($/kW). The overall UWMAK-III plant efficiency is expected to surpass the efficiencies of earlier UWMAK-I[5] (32%) and UWMAK-II[6] (36%) conceptual designs, and a goal of approximately 40% was selected. This means that a power cycle thermal efficiency of 43-44% will be required.

The upper limit of the UWMAK-III power plant performance is constrained by the blanket capability (i.e., temperature) rather than limitations imposed by helium gas turbine technologies. The current state-of-the-art helium gas turbine inlet temperature is between 760 C (1400 F) and 815 C (1500 F), and by the year 2010 this temperature is expected to increase approximately three to four hundred degrees. The thermal pollution problem attributable to power stations is becoming more serious and it can be expected that by the time fusion power generation becomes practical, the use of dry cooling for waste heat rejection may be imperative. A closed-cycle helium gas turbine power system will be economically more adaptable to dry cooling because heat rejection takes place over a temperature range much higher than the condenser temperature in a Rankine steam power system.

The two-zone (lithium/helium cooled) blanket design is certain to impose considerable constraints on the selection of the power cycle configuration, the number of turbomachinery loops, the unit capacities (identical or different), the integration schemes for the turbomachines, and the thermal storage system.

Breeding of tritum in the lithium coolant means that an intermediate heat exchanger is required to contain tritium and prevent significant diffusion into the power conversion loop. This results in a lower turbine inlet temperature that, in turn, reduces the power conversion efficiency. A helium gas turbine can be integrated directly with a helium-cooled blanket thus avoiding the above temperature loss, provided no tritium breeding is required in that blanket.

The UWMAK-III and any Tokamak fusion reactor have a unique operating cycle in which the "burning" of the fusion plasma has to be shut down periodically as discussed in section 3. While there is some flexibility in designing a burn cycle, a long-pulsed cycle with approximately 30 to 100 minutes burn time and 1 to 6 minutes downtime have been reported (refs. 5, 6, and 17). Since the power conversion system cannot tolerate even momentary cutoff from the heat source, a means to store thermal energy for use during every reactor downtime will be required. Theoretically, the power conversion system should not detect the reactor downtime but in reality the operation of the power conversion system can be complicated by provision of the thermal storage system.

From the power utility viewpoint, a fusion power plant must be capable of delivering uninterrupted constant-output 60 Hertz ac power under normal operating conditions. This would require that the turbomachines must operate at 3600 rpm, and that the operational characteristics of the power conversion systems must be adaptable to the existing power grids. Based on the power plant output level mentioned above, the two-zone blanket design, and the need to provide a reasonable system redundance, turbomachinery unit capacity of approximately 500 to 600 Mwe would be required. A summary of UWMAK-III power system requirements and constraints is given in Table 6.

TABLE 6

UWMAK-III POWER SYSTEM REQUIREMENTS AND CONSTRAINTS

1. Advanced Technology (Second Generation Fusion Power Plant)

2. High Performance (Surpass UWMAK I and II)

3. Dry Cooling Tower

4. Two-Zone Blankets

5. Acceptable Tritium Extraction and Containment

6. Around-the-Clock Operation with Thermal Storage

7. Compatibility with Helium/Lithium Temperature Rise in the Blankets and Heat Exchanger Loops

8. Moderate Maximum Helium Pressure (750 - 1000 psi), and Reasonable System Pressure Loss ($\sim 8\%$)

9. 3600-RPM Turbomachines/60 Hertz A-C Power

10. 1500 - 2000-Mwe Approximate Station Capacity

11. Acceptable Operational Characteristics

7. Parametric Performance Analyses

While the selection of the power cycle configuration is largely dependent
on the requirements or constraints imposed on the power conversion system (such
as type of heat source and heat rejection scheme among others,) the levels of
intercooling, regeneration, and reheat will have to be decided based on a trade-off
between the system performance and cost. Therefore, appropriate parametric
analyses were required to select the reference design system. Based on various
combinations for intercooling (none, one, or two), regeneration (none or regenerative),
and reheat (none or one), at least twelve different cycle configurations can
result. A preliminary screening was made and six of these configurations were
selected for further evaluation. The selection of cycle configuration and the
subsequent operating conditions for a given closed-cycle gas turbine (or any
baseload power system) is often dictated by the compatibility of the cycle with
the requirements and constraints imposed on the power conversion system and by
a trade-off between the cycle performance (i.e., efficiency) and the complexity
(i.e., costs) for generating the lowest cost electric power.

A baseline cycle configuration was selected using a "compatibility matrix",
as shown in Fig. 12, to check the capability of each of the six candidate
cycle configurations to meet nine of the power conversion system requirements
and constraints selected from Table 6. The results indicate that the
regenerated cycle with one intercooling stage would be most suitable for the
UWMAK-III power conversion and this was selected as the baseline cycle configuration
for further parametric analysis. Figure 13 shows a T-S diagram and a schematic
flow diagram for the baseline cycle configuration selected.

Crucial parameters which could significantly affect the power conversion
performance and/or equipment cost were identified and are listed in Table 7.

TABLE 7

UWMAK-III POWER CONVERSION CYCLE PARAMETERS

One Intercooling Stage, No Reheat

- Turbine Inlet Temperature

- Turbine Inlet Pressure

- Overall Pressure Ratio

- Regenerator Effectiveness

- Compressor Inlet Temperature

- System Pressure Loss

- Turbine Efficiency

- Compressor Efficiency

The turbine inlet temperature, which is always constrained by the blanket coolant outlet temperature, is the most significant parameter for the cycle thermal efficiency; 1500 F (815 C), 1600 F(871 C), 1800 F (982 C) and 2000 F (1093 C) were selected for parametric analyses based on the potential progress that can be expected in the development of blanket structural materials. A high turbine inlet pressure is desirable to obtain smaller power system equipment and better heat transfer coefficients; 1000 psia was selected as the reference point but sensitivity analyses were made for 750, 1500, 2000, and 3000 psia. Eight overall pressure ratios between 1.6 and 6.0 were considered as parametric points. The performance of the baseline cycle was analyzed for 0, 60, 70, 80, 90, and 100 percent regenerator effectiveness to examine their impact on the cycle thermal efficiency. Since dry cooling towers were specified for waste heat rejection, a compressor inlet temperature of between 80 and 140 F was considered. The level of system pressure loss increases with the increase of cycle complexity, and 6, 8,10 and 12 percent were selected as parametric points. An independent variation of all the parameters would result in over 15,000 design points which is beyond the scope of the current study. Therefore, some of the cycle parameters were varied only selectively to yield a manageable number of design points. Extensive parametric performance analyses were carried out for the baseline and some off-baseline cycle configurations to (1) reassure the suitablity of the baseline cycle configuration and (2) to generate sufficient data needed for subsequent trade-off studies.

The turbine inlet temperature is the single most important parameter which affects the thermal efficiency of the power conversion system. A maximum cycle thermal efficiency of nearly 44 percent at a turbine inlet temperature of 1600 F (871 C) and total pressure ratio of about 2.8 would lead to a station efficiency

of approximately 40%; the cycle thermal efficiency increases approximately
1.8 points per 100 F (56 C) increase in the turbine inlet temperature. While
the cycle thermal efficiency reaches a maximum value at an optimal pressure ratio
of about 2.8, the specific work continued to increase with the increase in
pressure ratio, indicating that the selection of the design point could be a
compromise between the thermal efficiency for system economy and the specific
work for large unit capacity. A trade-off between the cycle performance
improvement and the regenerator cost increment would be necessary, however.
A lower compressor inlet temperature is desirable for higher efficiency, but
this temperature is always constrained by the waste heat rejection scheme
available to the power plant. The cycle thermal efficiency drops by about
0.7 points per 10 F (5.5 C) increase in the compressor inlet temperature.
The effect of total pressure loss on the cycle performance was found to be an
approximately 0.8 point decrease in thermal efficiency per 1% increase in
pressure loss within the 6 to 12% range considered.

A comparison of cycle thermal efficiency for the baseline cycle with the
alternative cycles is depicted in Fig. 14. The simple and simple-intercooled
cycles are apparently not acceptable because of excessively low thermal efficiency.
The regeneration cycle (cycle #3) would be more adaptable to dry cooling, but
its modest 40% cycle efficiency would lead to a station efficiency of about
35%. The choice between adding intercooling or reheat to improve the regenerative
cycle would appear rather clear; intercooling offers greater improvement without
using expensive high-temperature heat exchangers. A combination of all three
features (i.e., regeneration, intercooling, and reheat) would offer an
attractive performance but its technical feasibility would be constrained by the
blanket capability, among other factors. Therefore, it can be concluded that

the baseline configuration selected earlier by using a compatibility matrix is technically sound. The selection of the final reference design conditions requires consideration of the interface and trade-off problems which are discussed in the following section.

8. Interface and Trade-Off Studies

A tokamak fusion power plant can be considered to consist of three major systems: a reactor, a thermal (or alternative) energy storage system, and a power conversion (heat engine-generator) system. The integration schemes for these systems capable of around-the-clock generation will be dependent on the reactor operating cycle and conditions, the blanket configuration and capability range, the tritium breeding and extraction methods, and the power conversion system characteristics. The operating conditions and the types of coolants used in the blanket, the heat exchanger loops, and the power conversion system are also important factors which influence the selection of integration schemes. The concept of a two-zone blanket, inner and outer, with different tritium breeding requirements, different types of coolants and exit temperatures and different thermal power loading, would certainly complicate the integration of a helium gas turbine power system with a UWMAK-III type fusion reactor. Some of the crucial interface problems for the power conversion systems are summarized in Table 8.

The decision to have a helium-cooled inner blanket without tritium breeding and a lithium-cooled outer blanket with tritium breeding would mean that the use of a primary heat exchanger to enable the containment and primary extraction of tritium within the lithium loop will be imperative (see Fig. 5 left and top diagram). If no intermediate loop is used, then the secondary loop of the primary heat exchanger and the inner blanket can be connected in

TABLE 8

CRUCIAL INTERFACE PROBLEMS

1. Integration Scheme (I/O Blanket - HX - CCGTs)

2. Temperature Compatibility

3. No. of CCGT/Unit Capacity

4. Tritium Inventory and Containment

5. Provision for Energy Storage

6. Material (Bimetal) Compatibility

7. Startup and Shutdown (Scheduled and Emergency)

8. Power Level Control

9. Scheduled Maintenance

10. Repairability

11. System Dynamics

series (Fig. 15 right and top), in parallel (not shown), or separately

(Fig. 15 right and bottom) with the helium gas turbine power systems. However,

the need for secondary extraction and/or stringent containment of tritium

and the need to store thermal energy using a liquid metal for the down part of

the burn cycle would require an intermediate sodium loop at a penalty of increased

temperature drop between the lithium coolant and the helium turbine inlet.

In this case, the inner and outer blankets can be connected in series

(Fig. 15 right and middle), in parallel (Fig. 15 left and middle) or

separately (Fig. 15 left and bottom) with the helium gas turbine power systems.

Since the inner blanket is "clean" with respect to tritium, the separate

connection scheme would be generally preferable. In this case, the split between

the inner and the outer blanket loading must be controlled such that the number

and capacity of the gas turbine loops is acceptable from the economic and

operational points of view.

The turbine inlet temperature and pressure and the regenerator high-

pressure-side outlet temperature are the only three thermodynamic properties

seen by the reactor blankets. Thus, they are important integration parameters.

The regenerator effectiveness and the overall cycle pressure ratio are indirect

parameters. Table 9 summarizes these critical integration parameters, the

trade-offs required, and the physical constraints imposed in selecting their

values. The selection of the critical integration parameters will have to be

based on performance-cost trade-offs while ensuring that the many physical

constraints inherent to power plant components are satisfied. Figure 16 shows

that for a turbine inlet temperature of 1600 F (871 C), the possible regenerator

exit temperature will be between 830F (443 C) to 1030 F (554 C) based on an

TABLE 9

CRITICAL INTEGRATION PARAMETERS

	Trade-off	Constraints
Direct		
TIT	η vs $	Blanket Outlet Temp. Material Capability
TIP	Size vs $	Seals, Material Strength Flow Path Heat Transfer
Regenerator Outlet Temp.	- - -	Blanket Inlet Temp. Flow Rate
Indirect		
Regenerator Effectiveness	η vs $	$\Delta P/P$
Overall Press Ratio	η vs Sp. Power	Critical Tip Speed

overall pressure ratio of between 2.25 and 3.0 and a regenerator effectiveness of 80 to 90 percent.

The turbine inlet temperature, which is the most important parameter for the power conversion efficiency, is constrained by the blanket coolant outlet temperature and the total temperature drop across the heat exchangers. For a given blanket coolant exit temperature, a higher turbine inlet temperature can be obtained by using higher heat exchanger effectiveness (thus larger size), thus indicating that a trade-off between system performance and heat exchanger cost will be required. This temperature drop is in the 80-200 F (27-93 C) range depending on whether an intermediate heat exchanger is used. Note that the use of a lithium (blanket coolant) to helium (working fluid) heat exchanger still constitutes a "direct" cycle integration because of the volumetric heat generation by neutron capture within the lithium itself. However, if tritium breeding is not necessary, such as in the case of the inner blanket, direct integration is desirable to achieve the highest power conversion efficiency for a given blanket outlet temperature, simplicity of integration and possibly lower power generation costs. Past component and design studies for 100 to 600 MWe closed-cycle gas turbine power systems and their performance and cost characteristics were utilized in selecting a reference design regenerator of 88% effectiveness.

The reference design conditions for the baseline cycle configuration were selected based on interface problems and preliminary trade-off considerations. The temperature and pressure for the major cycle points are identified in the cycle flow diagram shown in Fig. 17. The turbine inlet temperature of 1600 F (871 C) was selected essentially based on projected blanket capabilities with consideration given to the heat exchanger temperature drops and the projected

turbomachinery technology. As pointed out earlier, the limiting factor is the blanket outlet temperature and thus the selection of the turbine inlet temperature involved system constraints more than trade-offs. The compressor inlet temperature of 100 F (43 C) was selected based on the dry cooling tower requirement and reasonable precooler and intercooler designs. Despite the dry tower cooling, the use of intercooling to gain more than three points in cycle efficiency is justified considering the potential saving in power generation cost over the lifetime of the fusion plant versus the capital cost of the intercooler.

The selection of the turbine inlet pressure is largely based on component sizes and heat transfer considerations. As will be mentioned later, use of 1000 psia inlet pressure was mandatory for a turbomachinery unit capacity in the 500 to 600 MWe range. The overall pressure ratio of 2.8 (or 2.6 for turbine) was selected for a maximum cycle efficiency, and the intercooling pressure was selected so that the compressor work required will be a minimum. The regenerator effectiveness of 88% represents a compromise to accomodate the integration constraints yet generally provide a balance between the system performance and costs. Based on the operating conditions specified in Fig. 17, the cycle efficiency is estimated to be 43.9%, thus allowing an overall plant efficiency of greater than 40%.

9. Conceptual Design of Closed-Cycle Gas Turbine Power Systems

In designing the power system arrangment, the first question to be answered is the number of power conversion loops needed and the unit capacity for each loop. Utilization of multiple units of a standardized power conversion system arrangement often leads to component capital cost reduction as well as easy operation, maintenance, and repair. However, a major disadvantage of the multiunit arrangement is the complex governing and valving systems needed to run individual turbomachinery. Therefore, the total number of branched turbomachinery

units should be limited to 3 or 4, if possible. A first glance at the thermal power rating of the UWMAK-III fusion reactor (5000 MW$_t$) would suggest that between 3 and 6 units of helium turbomachinery would seem appropriate. Further examination of the inner (helium) and outer (lithium) blanket temperature capabilities and the possible thermal power split would narrow down the number of inner and outer blanket turbomachine units to 1+2 (1 for the inner blanket, 2 for the outer blanket), 1+3, 2+4, and 2+6 using a direct-cycle for the inner blankets. After more detailed examination on blanket and turbomachinery design characteristics, the 1+2 system arrangement using three identical 585 MW$_e$ power conversion systems was selected based primarily on the projected turbomachinery technology and economic considerations.

The finalized system arrangement for the UWMAK-III fusion power plant is shown in Fig. 18. During each 30 minute "burntime", the No. 1 and No. 2 power conversion systems will draw thermal energy from the outer blanket through the primary (lithium to sodium) and the secondary (sodium to helium) heat exchangers at a turbine inlet temperature of 1600 F (871 C). The No. 3 power conversion system will be directly integrated with the inner blanket and thus also operate at the same turbine inlet temperature. During the burn time, the sodium thermal storage system will be "charged" to store sufficient thermal energy to operate all three power conversion systems during the subsequent 1.5 minute "downtime," During the downtime, the thermal storage system will be "discharged" through the same sodium-helium heat exchanger to operate the No. 3 unit. Operating temperatures and flow rates for key points in the inner and outer blanket heat transfer loops are also identified in Fig. 18.

For a given rotation speed and operating temperature, the physical size of the turbomachinery is often limited by the maximum diameter of the last turbine

stage where the maximum volume flow requires a maximum blade length, thus
resulting in maximum stress levels (tensile and bending). In the compressor
and turbine blade designs, it is desirable to use the highest possible speed
with an optimum hub-to-tip ratio. For the larger turbomachinery units, the
optimum speeds for the compressors are lower, and past experience indicates
that for unit capacities of about 200 MWe and larger, the single shaft con-
figuration is preferable. In some cases, use of a double-flow turbine may be
necessary (particularly for a low pressure unit) to accommodate the large
volume flow in a single shaft turbomachinery design. Single-shaft turbomachinery
designs as large as 1200 MWe rating have been reported[20,21] and there seems
to be no inherent mechanical limitation for such large turbomachinery.

The reference design 585-MWe turbomachinery (3 needed) for the UWMAK-III
fusion power plant was based on a single-shaft, single-flow configuration
at 3600 rpm shaft speed. This single-shaft turbomachinery can be coupled
directly to the alternator to avoid overspeed, and generally represents a
fairly compact design without serious penalties in the performance of the
compressors. Generally speaking, the turbomachinery can be designed for
either maximum efficiency or maximum output (per unit weight or volume) or
somewhere between. The present design is for maximum efficiency based on 50%
reaction at the mean diameter flow and a flow coefficient of approximately 0.5.
Based on the unit capacity and rpm specified, the current design using one
intercooler is regarded as the best promise satisfying the power plant requirements
and constraints summarized in Table 6.

The design data for the turbomachinery are summarized in Table 10, and Fig. 19.
depicts the turbomachinery structure, including the arrangement of compressors
and turbine, bearings and seals, and the overall dimensions. While conventional
seals are regarded as sufficient for internal sealing, hermetic seals may be

TABLE 10

CLOSED-CYCLE GAS TURBINE TURBOMACHINERY SUMMARY

Reference Design
585-Mwe Unit Output (3 units needed)

	Low Compressor	High Compressor	Turbine
Inlet Temperature - F	110	110	1600
Outlet Temperture - F	258	259	1000
Inlet Pressure - psia	380	640	1000
Outlet Pressure - psia	640	1080	380
Pressure Ratio	1.68	1.69	2.63
Efficiency (Adiabatic) - %	89	89	91
Number of Stages	10	10	9
Work per Stage - Btu/lb	18.6	18.9	75.1
Helium Flow - lb/sec	1472	1472	1472
Hub Diameter - in.	65	65	65
Inlet Tip Diameter - in.	79.7	73.9	79.8
Outlet Tip Diameter - in.	76.1	71.8	92.8
Wheel Speed, Hub - ft/sec	1021	1021	1021
Maximum Tip Speed	1251	1160	1458
Shaft Speed - rpm	3600	3600	3600

needed for the end seals. Because of the large flow area required at the turbine

exit, an axial-flow flange design was adopted. The turbomachinery has the unique

cost saving feature of employing the same constant hub diameter for the turbine and

the compressors, all on the single shaft. The maximum diameter and blade length are

92.8 and 13.9 in. (235.7 and 35.3 cm), respectively, and the stresses resulting from

these configurations are regarded as well within the projected material capabilities.

Since the heat transfer coefficients are not too different between the

high- and low-pressure sides, straight unfinned tubes were selected as

the basic heat transfer surface to minimize hot- and cold-side pressure losses.

Based on the operating conditions for the regenerator as defined in Fig. 17,

preliminary design studies showed that a simple counter flow regenerator with

a single tube-pass offers a good compromise between performance and cost,

particularly by utilizing standardized heat exchanger modules. The heat

exchanger module, which is somewhat similar to the fuel element concept used

in the light water reactors, would consist of 100 small heat transfer tubes arranged

at 1 in. (2.5 cm) pitch inside a 10-in. by 10 in. (25 cm by 25 cm) rectangular can, as

shown in Fig. 20. The tube bundle merges to a single "conductor" tube at both

ends of the heat transfer element. The heat transfer elements are then stacked

up inside the regenerator shell while the connector tubes are welded to the inlet

and outlet headers, as shown in Fig. 21. The high-pressure "cold" helium will

flow inside the tubes while the low-pressure "hot" helium will flow outside the

tube bundles, through the heat exchanger cans inside the regenerator shell. The

reference-design regenerator has an inner shell diameter of 13 ft. (396.2 cm) and an

overall shell length of 75 ft. (2286 cm); the effective tube length is 59 ft. (1798 cm)

as shown in Fig. 21. The details of the regenerator design data are summarized in

Table 11. The regenerator would require 150 heat exchanger elements which would

result in a reasonable pressure loss for the helium flow rate required.

TABLE 11

HEAT EXCHANGER DESIGN DATA SUMMARY

Reference Design

	Regenerator	Precooler	Intercooler
Heat Rate - Btu/hr	4.31×10^9	1.57×10^9	9.81×10^8
Flow Rate - lb/hr			
Hot Side (Helium)	5.324×10^6	5.324×10^6	5.324×10^6
Cold Side	5.324×10^6	1.5×10^7 water	9.34×10^6 water
Pressure Loss, $\Delta P/P = \%$			
Hot Side	2.8	1.3	1.1
Cold Side	1.0	---	---
Effectiveness - %	88	92	88
Overall Heat Transfer			
Coefficient - Btu/hr-ft^2-F	343	438	346
Heat Transfer Area - ft^2	1.41×10^5	6.95×10^4	5.97×10^4
Number of Heat Exchange Elements	150	150	150
Effective Tube Length - ft	58	36	31
Overall Shell Length - ft	75	48	42
Approximate Weight - ton	185	115	100

The general design concept of the regenerator is also applicable to the precooler and intercooler except that smaller tubes will have to be used to yield an outer/inner (i.e., helium/water) flow area ratio of about 7.5. The tube diameter in this case will be 0.37 in.(.94 cm) instead of 0.545 in.(1.38 cm) for the regenerator design. The heat exchanger element design data for the precooler as well as the intercooler are tabulated in Fig. 20. Cooling water inlet temperature of 90 F (32 C) and outlet temperature of 195 F (91 C) were used for both the precooler and the intercooler. Pressurization would be necessary in order to prevent local boiling of cooling water. However, the cooling water pressure must be maintained below the helium pressure so that in the event of a tube leak no moisture will leak into the helium loop. Table 11 also summarizes the design data for the precooler and the intercooler while the shell diameters, effective tube lengths, and overall shell length of these elements are shown in Fig. 21 for comparison with the regenerator.

The piping system sizes for connecting the power conversion system components were estimated based on reasonable flow velocities for the flowing fluid at the existing temperature and pressure. The results are tabulated in Table 12. The layout of the power system components must be arranged to reduce the pipe length and to minimize pipe bends. This is to reduce both the piping cost and to avoid excessive pressure loss in the piping systems. The largest pipe size required will be 8.87 ft.(269 cm) in diameter connecting the turbine exit with the regenerator while the smallest pipe will be 2.5 ft. (76 cm) in diameter for cooling water flow to the precooler and intercooler. Figure 22 shows the relative locations and layout for the major power system components and the overall dimensions of the conceptual UWMAK-III fusion power station.

TABLE 12

PIPING SYSTEM DESIGN DATA SUMMARY

Reference Design

From	To	Fluid	Temp., F	Press., psia	Diameter
Turbine exit	Regenerator	Helium	1000	380	8'10"
Regenerator	Precooler	Helium	348	380	6'6"
Precooler	Low Compressor	Helium	110	380	5'6"
Low Compressor	Intercooler	Helium	258	640	5'0"
Intercooler	High Compressor	Helium	110	640	4'6"
High Compressor	Regenerator	Helium	259	1080	4'2"
Regenerator	Blanket or Heat Exchanger	Helium	911	1000	5'6"
Blanket or Heat Exchanger	Turbine Inlet	Helium	1600	1000	6'6"
- -	Precooler Inlet	Water	90	15	3'0"
Precooler Outlet	- -	Water	195	15	3'0"
- -	Intercooler Inlet	Water	90	15	2'6"
Intercooler Outlet	---	Water	195	15	2'6"

10. Conclusions

The conceptual UWMAK-III fusion power plant utilizing closed-cycle helium gas turbines would offer an attractive station efficiency (about 42%) surpassing that of UWMAK-I[5], UWMAK-II[6] and the Princeton fusion plant design[17], without requiring cooling water supply for waste heat rejection. The cycle configuration most suitable for UWMAK-III power conversion would require single intercooling with regeneration (88%) operating at 1600 F (871 C) and 1000 psia helium turbine inlet conditions. Direct integration of a closed-cycle gas turbine with the helium-cooled inner blanket offers considerable advantages in terms of power conversion efficiency. However, integration with the lithium-cooled outer blanket where tritium breeding is accomplished will require a primary and most likely an intermediate heat exchanger. This necessitates a higher blanket coolant outlet temperature for the same turbine inlet temperature. A thermal power split of one-to-two between the inner and outer blankets, respectively, would permit utilization of three identical power conversion loops of 585 MWe each, representing a well-balanced power system integration arrangement.

Although a single-shaft turbomachine designed for 585 MWe output would result with the three-loop power system arrangement, unit capacities as large as 1000 MWe would appear technically possible; at least two power loops will be needed for UWMAK-III. Preliminary heat exchanger design studies indicate that use of standardized heat exchanger modules containing unfinned tube bundles with simple counterflow arrangement could result in compact regenerator, precooler, and intercooler designs that have reasonable pressure loss characteristics. The need for thermal energy storage appears imperative for around-the-clock power generation because of the inherently cyclic nature of Tokamak plasma operation.

Failure to develop a viable energy storage system could hamper the implementation of UWMAK-III or any long-pulsed Tokamak fusion power plant.

The principal advantages of closed-cycle helium gas turbines for fusion power generation include: (1) attractive thermal efficiency at moderate temperature, (2) compact turbomachinery with large unit capacity, (3) simple component designs, (4) adaptability to dry cooling tower, (5) working fluid inert to radioactivity, and (6) potentially low capital costs. Potential improvement in UWMAK-III power plant efficiency via the use of higher turbine inlet temperatures would be constrained by the temperature capabilities of the blanket material rather than the turbomachinery. It is anticipated that increasing application of closed-cycle gas turbines for fossil, fission, and solar power generation will be realized and that the technological progress resulting from these developments will be directly applicable to fusion power systems.

ACKNOWLEDGEMENTS

References

1. R. W. Conn, G. L. Kulcinski and C. W. Maynard, "The UWMAK-II Study: A Conceptual Design of a Helium Cooled, Solid Breeder, Tokamak Fusion Reactor System", <u>Nucl. Eng. and Design</u>, (this issue).

2. B. Badger et al., "UWMAK-III, A High Performance, Noncircular Tokamak Power Reactor Design", Nuclear Eng. Dept. Report FDM-150, The Univ. of Wisc.-Madison, to be published.

3. T. Ohkawa, T. H. Jensen, Plasma Physics <u>12</u>, 789 (1970).

4. T. Yang and R. W. Conn, "MHD Equilibrium and Stability Calculations for a Noncircular, High β_θ Tokamak Plasma", Bull. Amer. Phys. Soc. <u>20</u>, 1280 (1975).

5. B. Badger et al., "UWMAK-I, A Wisconsin Toroidal Fusion Reactor Design", Nuclear Eng. Dept. Report FDM-68, The Univ. of Wisc.-Madison, Nov. 1973 (Vol. 1); May 1975 (Vol. 2).

6. B. Badger et al., UWMAK-II, A Conceptual Tokamak Power Reactor Design", Nuclear Eng. Dept. Report FDM-112, The Univ. of Wisc.-Madison, Dec. 1975.

7. R. W. Conn, G. L. Kulcinski, H. Avci, M. El-Maghrabi, Nuclear Technology <u>26</u>, 125 (1975).

8. See several University of Wisconsin Reports - G. L. Kulcinski, R. W. Conn, H. Avci, D. K. Sze, UWFDM-127; R. W. Conn, D. K. Sze, UWFDM-128; G. L. Kulcinski, H. Avci, UWFDM-135.

9. W. Young and R. W. Boom, Chapter 4 of Ref. 2.

10. H. Segal, T. G. Richard, "Low Temperature Resistance Studies on Cyclically Strained Aluminum", Proc. Cryogenic Eng. Conf. (Kingston, Ca., July 1975), to be published in <u>Advances in Cryogenic Engineering</u> (Vol. 21)

11. R. W. Conn, Y. Gohar and C. W. Maynard, "Neutron Transport Calculations in a Torus", Trans. Amer. Nucl. Soc. (June 1976) to be published.

12. G. L. Kulcinski, J. W. Davis, R. E. Schmunk, "The Case for Molybdenum Alloys in D-T Fusion Reactors", Nuclear Engineering Dept. Report FDM-142 (Univ. of Wisc., Nov. 1975).

13. R. J. Bickerton, J. W. Connor and J. B. Taylor, Nature <u>229</u>, 110 (1972).

14. R. Behrisch and B. B. Kadomtsev, in <u>Plasma Physics and Controlled Nuclear Fusion Research, 1974</u> (IAEA, Vienna, 1975) Vol. II, p. 229.

15. D. K. Sze, (private communication).

16. D. K. Sze and I. Sviatoslavsky, Chapter 6 of Ref. 2.

17. R. G. Mills, ed. "A Fusion Power Plant", Princeton Plasma Physics Lab Report MATT-1050, Princeton University, Aug. 1974.

18. S. C. Kuo, "Solar-Powered Closed-Cycle Gas Turbine", Paper presented at the 9th IECEC, August 26-30, 1974, San Francisco, California.

19. S. C. Kuo, "Nuclear Gas Turbine Power Systems", United Technologies Research Center Report N-150967-2, October 1974.

20. W. Enders, "Large Helium Turbines for Nuclear Power Plants", ASME Paper 70-GT-99, May 1970.

21. K. Bammert, E. Bohm, "Nuclear Power Plants with High Temperature Reactor and Helium Turbine", ASME Paper 69-GT-43, March 1969.

Figure Captions

Fig. 1 — Overall cross section view of the conceptual tokamak fusion power station, UWMAK-III.

Fig. 2 — Cross section view of the right half of the torus in UWMAK-III showing the plasma, the blanket and shield, the main toroidal field magnets, the transformer and vertical field coils, and the vacuum pumping system.

Fig. 3 — Comparison of the plasma and toroidal field magnet size in UWMAK-III to the previous conceptual design, UWMAK-II.

Fig. 4 — Schematic of the blanket and shield design for UWMAK-III.

Fig. 5 — Essential features of the poloidal magnetic divertor including the location of the separatrix, the various coil systems, the particle collector plates, and the cryopumping system.
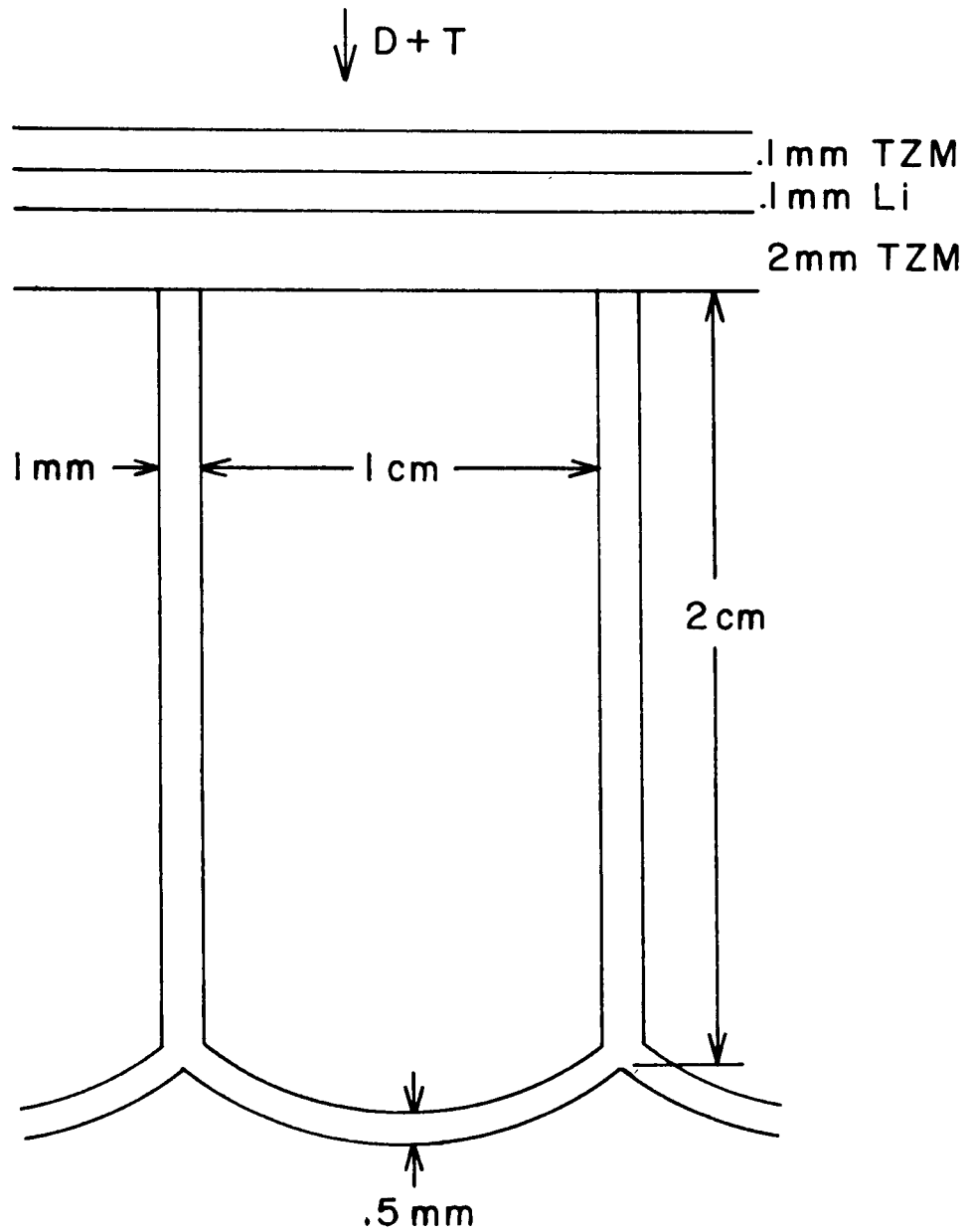
Fig. 6 — Schematic of the particle collector plate system design.

Fig. 7 — Cross section of the particle collector plate system showing the 0.1 mm lithium buffer layer and the 1 cm x 2 cm channels for sodium coolant flow.

Fig. 8 — Blanket model used for the two dimensional neutron and gamma transport calculations.
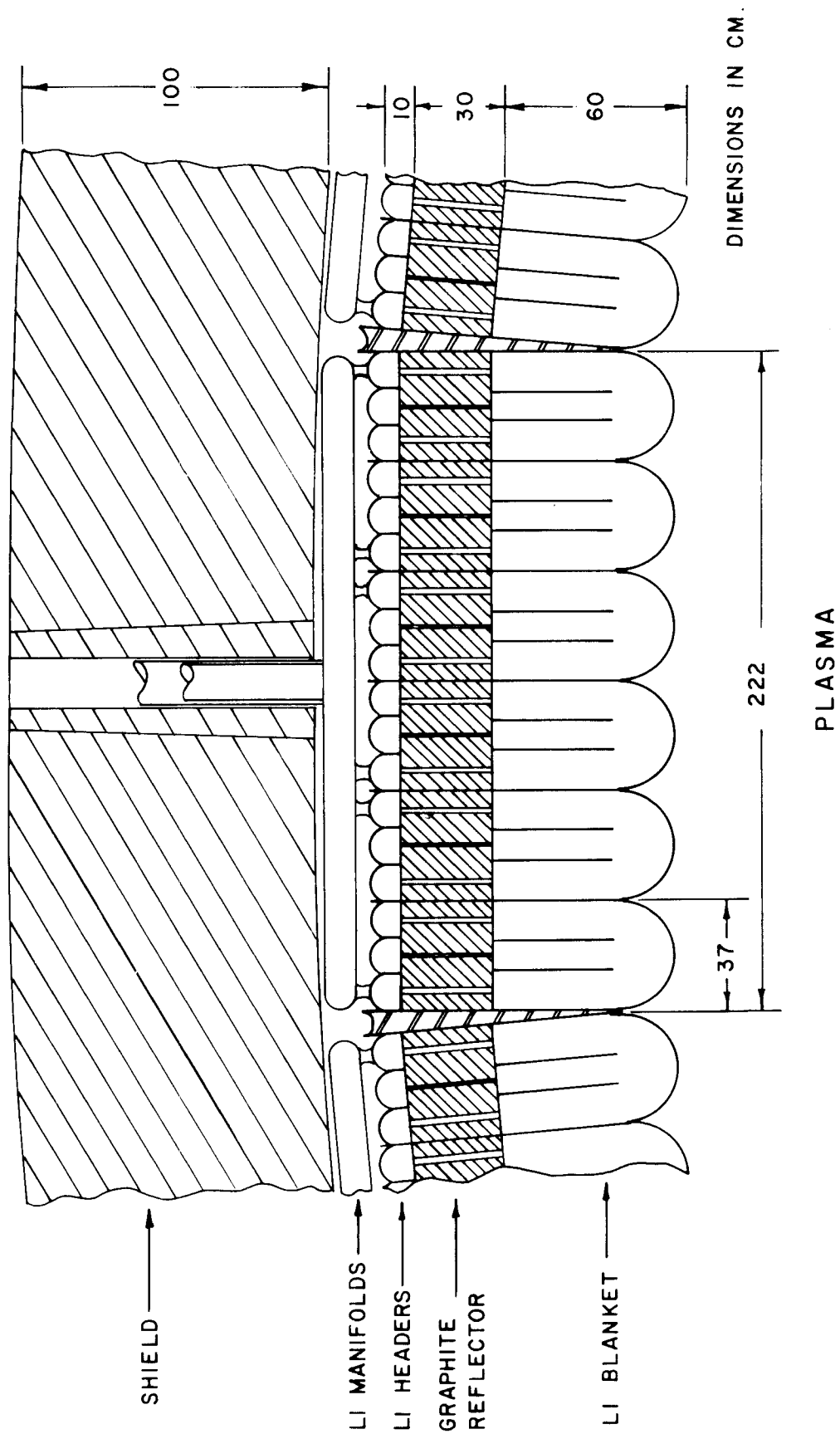
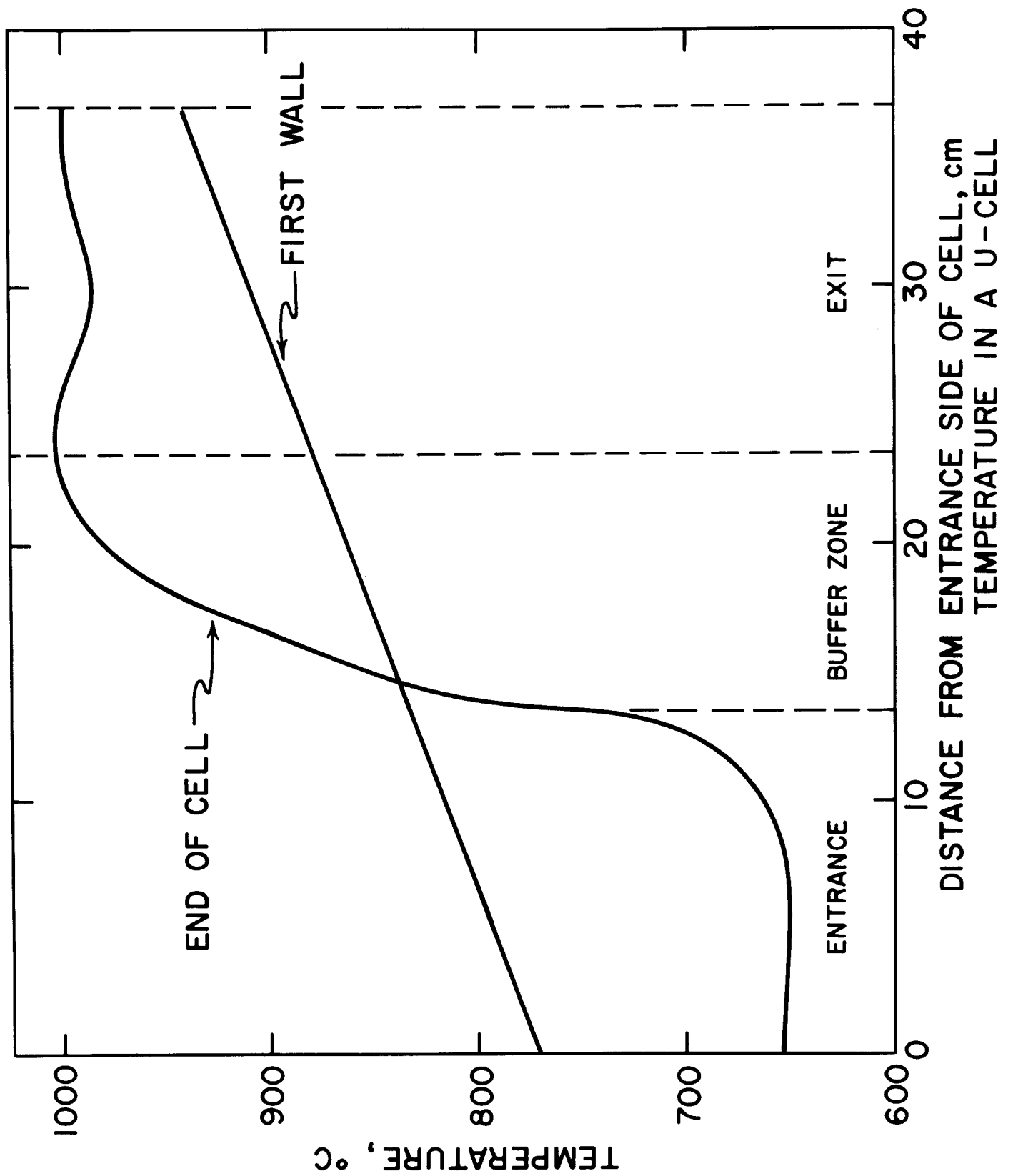Fig. 9 — Cross section of outer blanket and shield viewed in the toroidal direction.

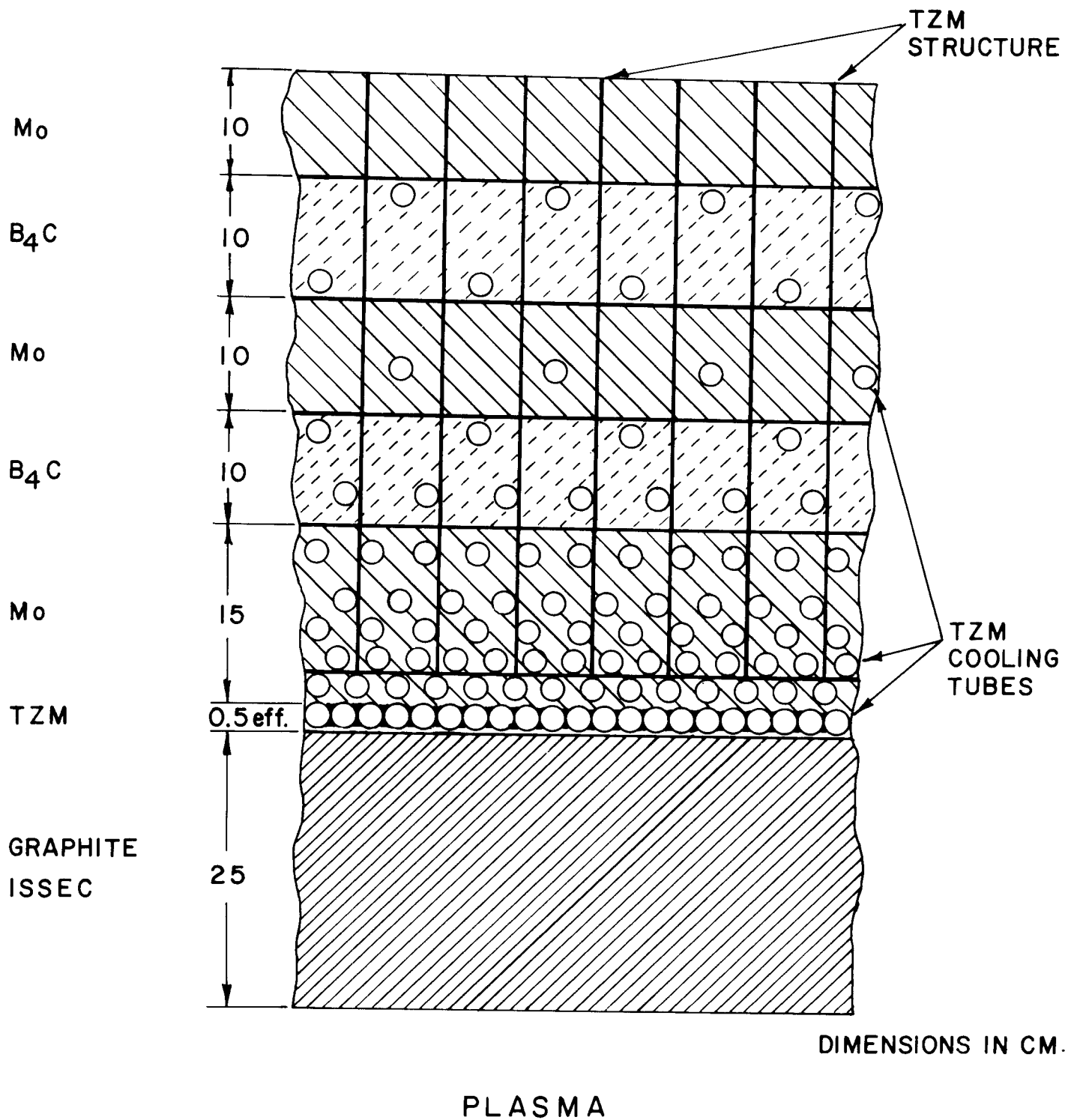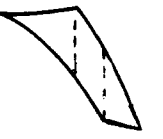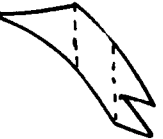Fig. 10 — Temperature distribution across a typical U-bend cell of the outer blanket.

Fig. 11 — Cross section of the inner hot shield showing the 25 cm graphite zone, which is not actively cooled. It serves to protect the inner first wall of TZM cooling tubes from radiation damage.

Fig. 12 — Closed cycle gas turbine selection matrix used for UWMAK-III.

Fig. 13 — Cycle diagram of the helium gas turbine system.

Fig. 14 — Closed cycle helium gas turbine performance assuming 1600 F (871 C) turbine inlet temperature.

Fig. 15 — Various integration schemes for the UWMAK-III power conversion system.

Fig. 16 — The outlet range for the regenerator as a function of the overall pressure ratio assuming the turbine inlet temperature is 1600 F (871 C).

Fig. 17 — Reference design of the closed cycle helium gas turbine system for UWMAK-III. Three identical loops would be required.

Figure 1 – Cross section view of the UWMAK-III conceptual
tokamak power reactor

CROSS SECTION VIEW OF UWMAK Ⅲ

Figure 2 - Cross section view of the right half of the nuclear island in UWMAK-III. The system is toroidal and therefore symmetric about the vertical axis.
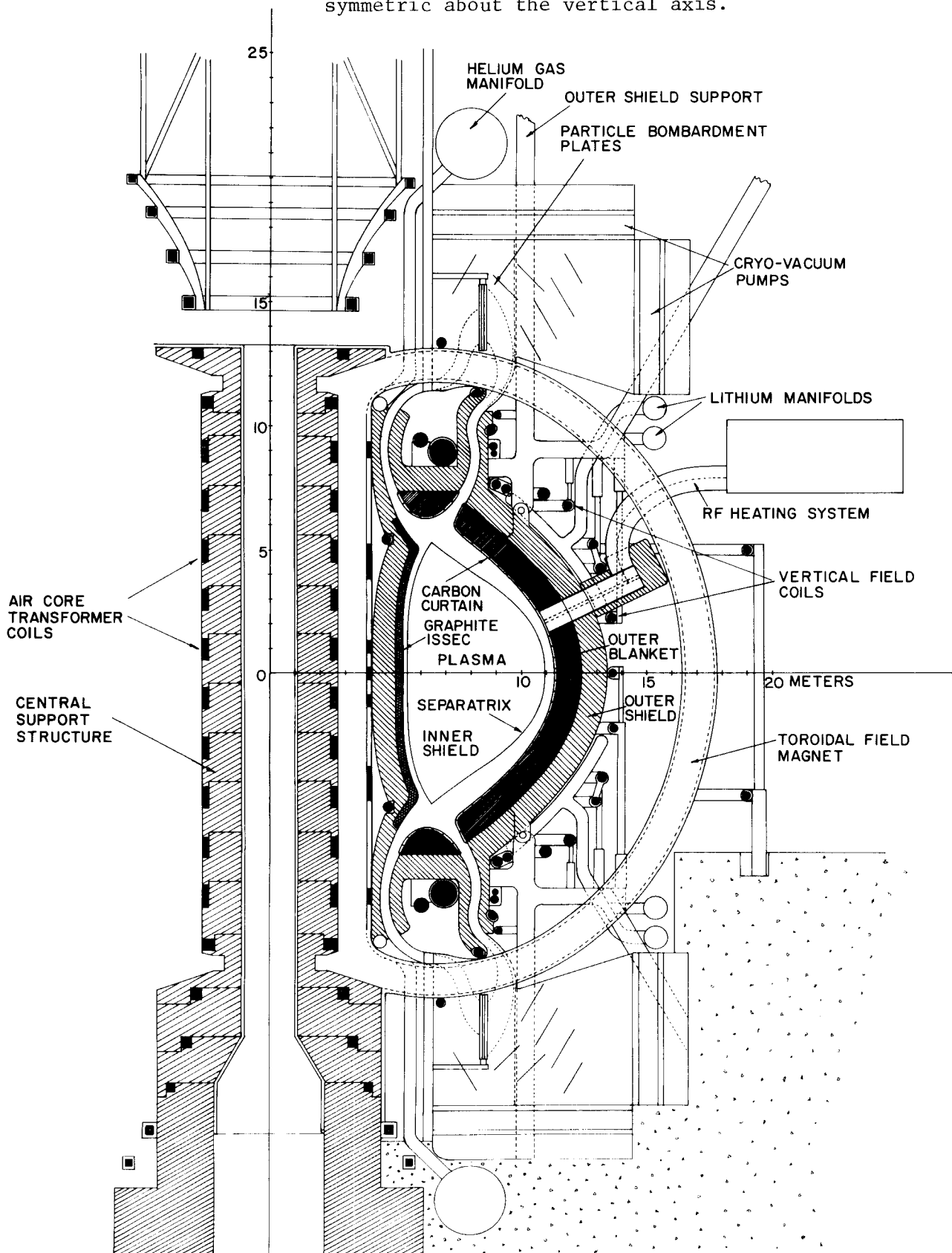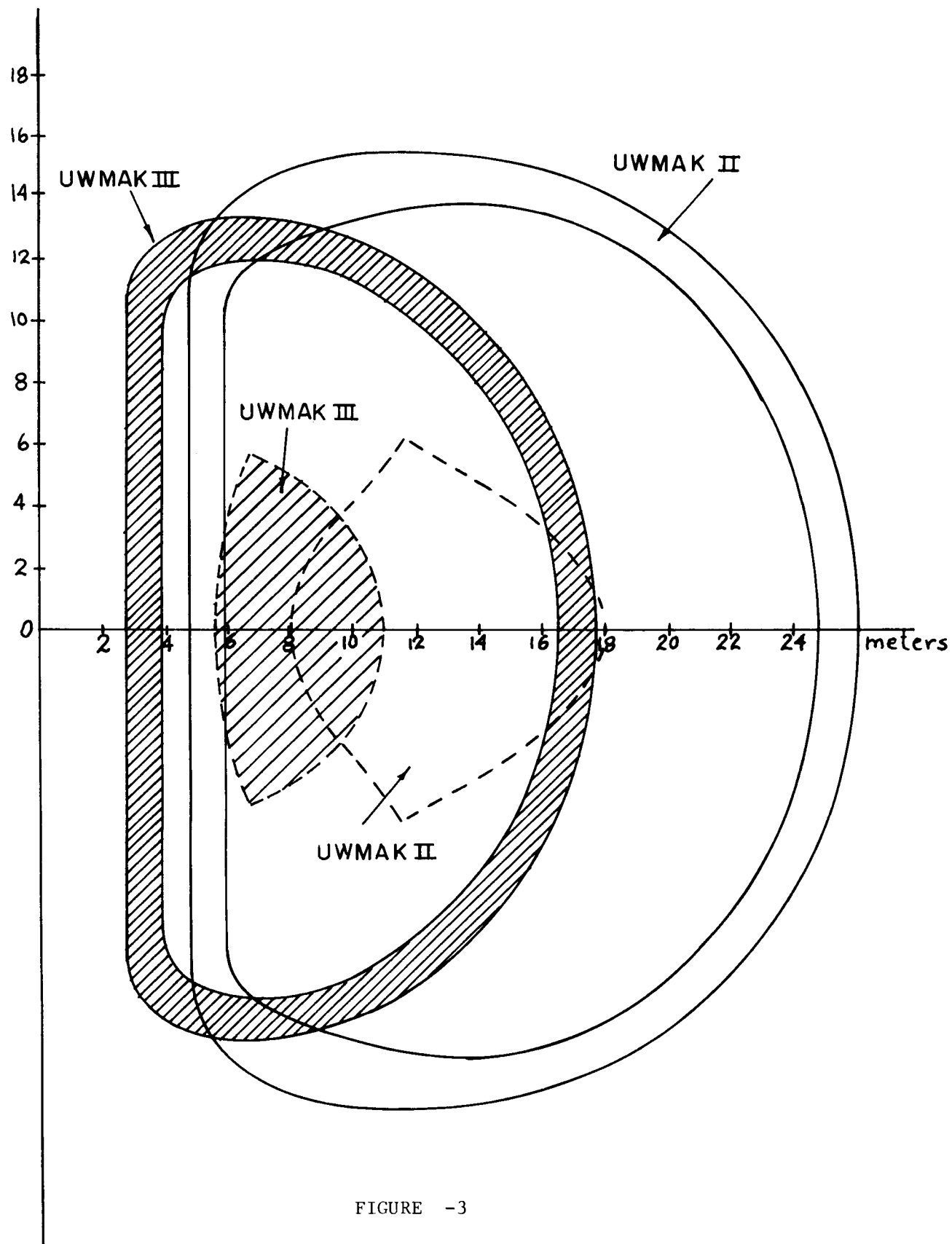
FIGURE -3

Comparison of the plasma and toroidal field magnet size in
UWMAK-III to the previous conceptual design, UWMAK-II.
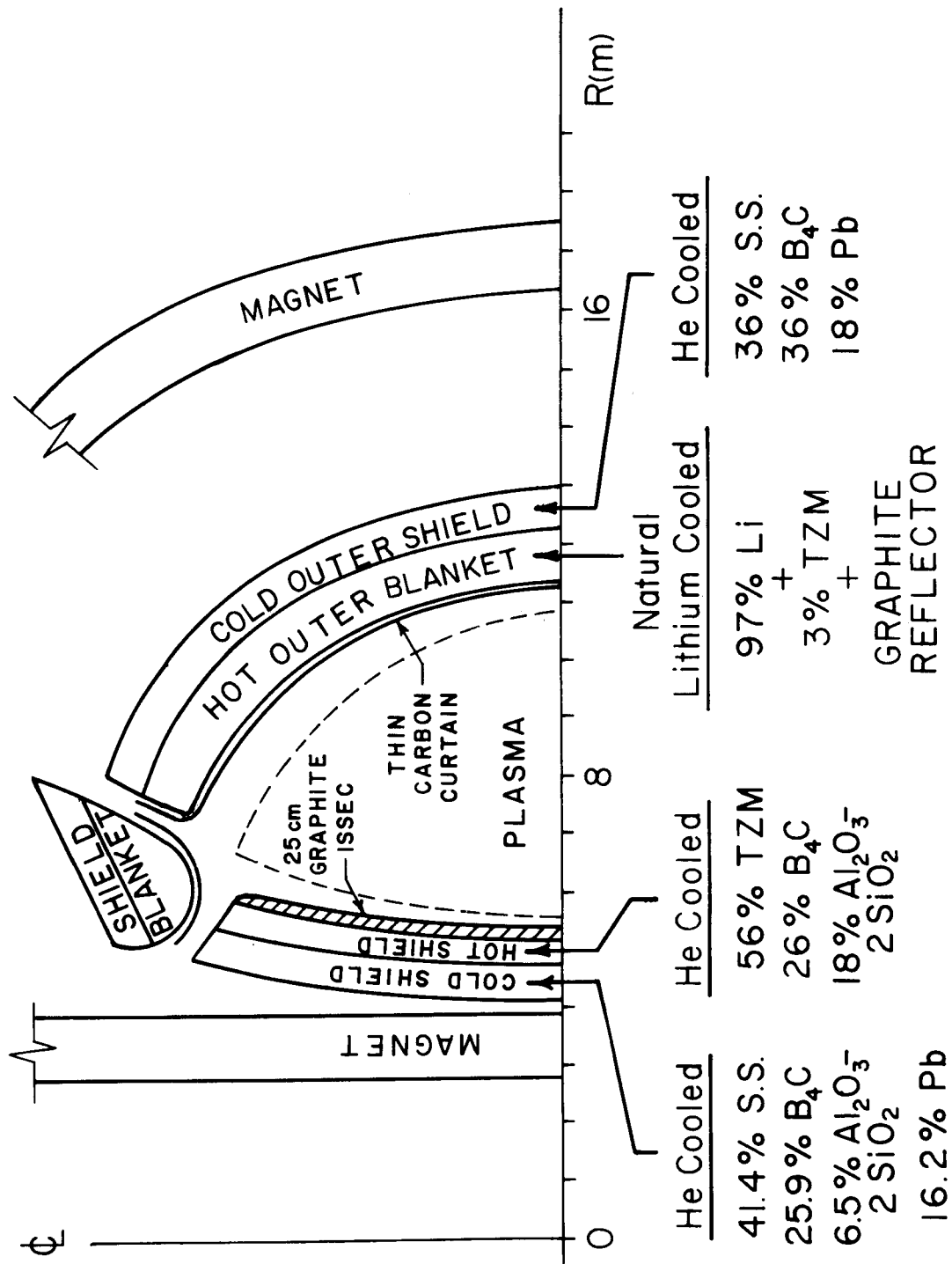
Figure 4 – Schematic of the blanket and shield design for
        UWMAK-III.
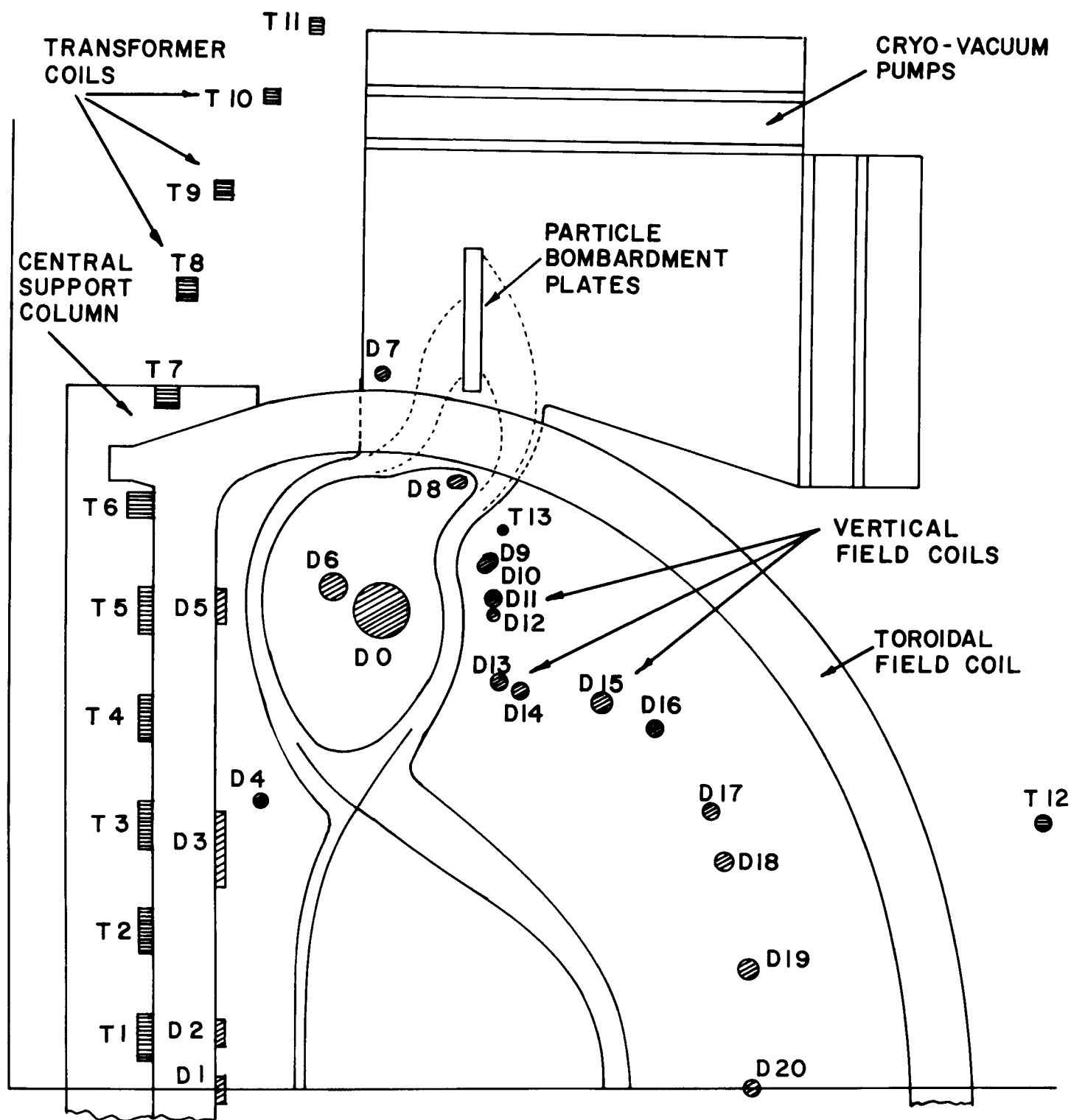
Figure 5 - Essential features of the poloidal magnetic divertor including
the location of the separatrix, the various coil systems, the
particle collector plates, and the cryopumping system.

SCHEMATIC DRAWING OF THE COLLECTOR
PLATE DESIGN FOR UWMAK III

SUPPLY ROLLER

FROZEN SEAL

COOLANT CHANNELS

SPENT ROLLER
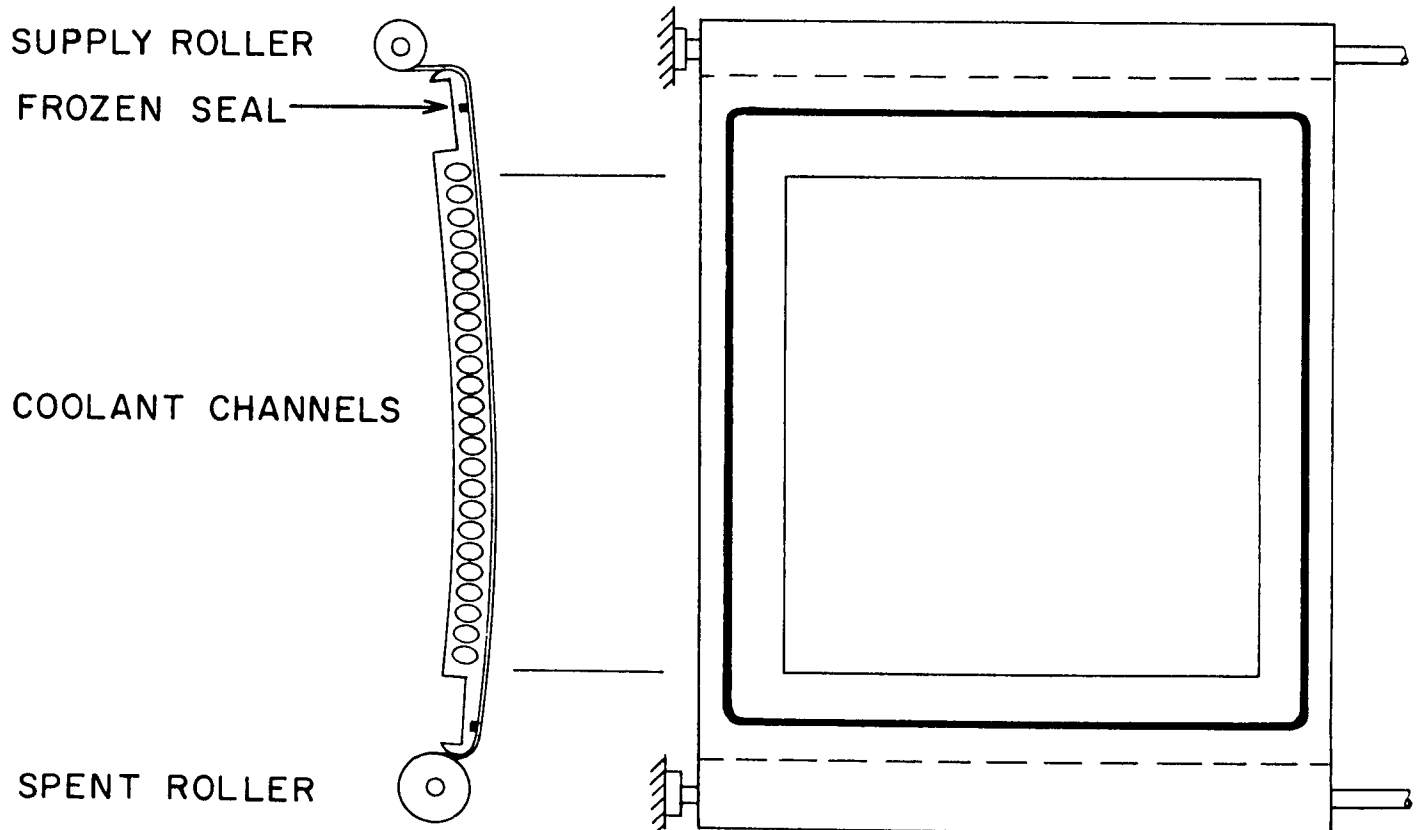
Figure 6 – Schematic of the particle collector plate system design

CROSS SECTION OF COLLECTOR PLATE

Figure 7 - Cross section of the particle collector plate system showing the 0.1 mm lithium buffer layer and the 1 cm x 2 cm channels for sodium coolant flow.

BLANKET MODEL USED FOR TWO-DIMENSIONAL NEUTRONICS ANALYSIS OF UWMAK-III
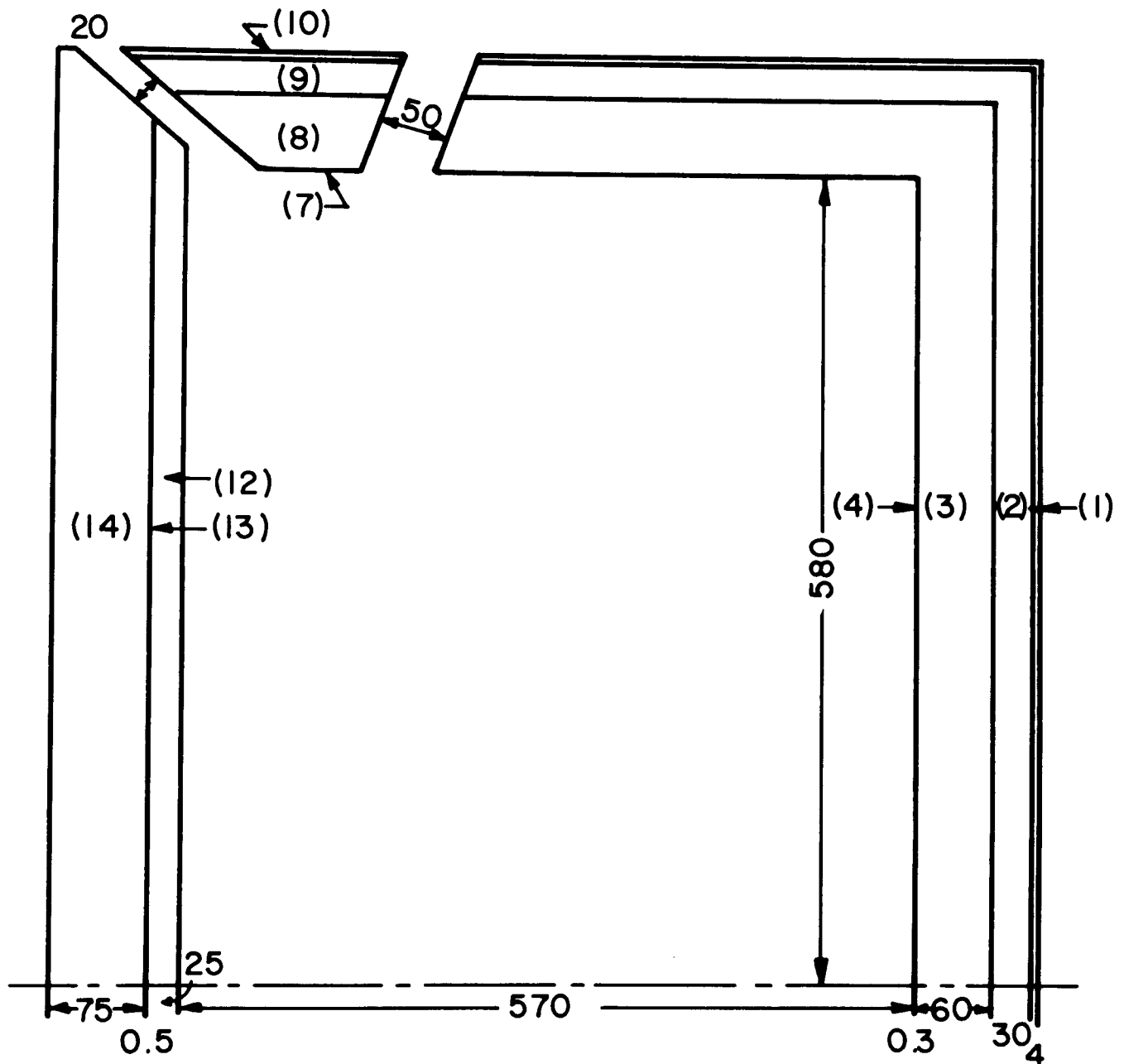
Figure 8 – Blanket model used for the two dimensional neutral and gamma transport calculations.

Figure 9 – Cross section of outer blanket and shield viewed in the
toroidal direction.

Figure 10 - Temperature distribution across a typical U-bend cell of the outer blanket.

Figure 11 — Cross section of the inner hot shield showing the 25 cm
graphite zone, which is not actively cooled. It serves
to protect the inner first wall of TZM cooling tubes from
radiation damage.

CCGT CYCLE CONFIGURATION SELECTION MATRIX
(UWMAK—III)

REQ. OR CONSTRAINT \ CYCLE CONFIG.	1	2	3	4	5	6
1. ADV. TECH.	X	√	O	O	O	O
2. HIGH PERFOR.	X	√	O	O	O	O
3. DRY TOWER	O	O	√	√	X	X
4. 2x BLANKET	√	√	√	√	√	O
5. THERM. STORAGE	?	?	?	?	?	?
6. He ΔT	X	O	O	O	O	O
7. P_{max} & ΔP	√	O	O	√	√	X
8. 3600 rpm/60 Hz	O	O	√	√	√	√
9. 2000—Mwe	X	√	O	O	O	O

O GOOD   √ FAIR   X POOR

Figure 12 – Closed cycle gas turbine selection matrix used for
UWMAK-III.

CYCLE DIAGRAM OF HELIUM GAS TURBINE SYSTEM
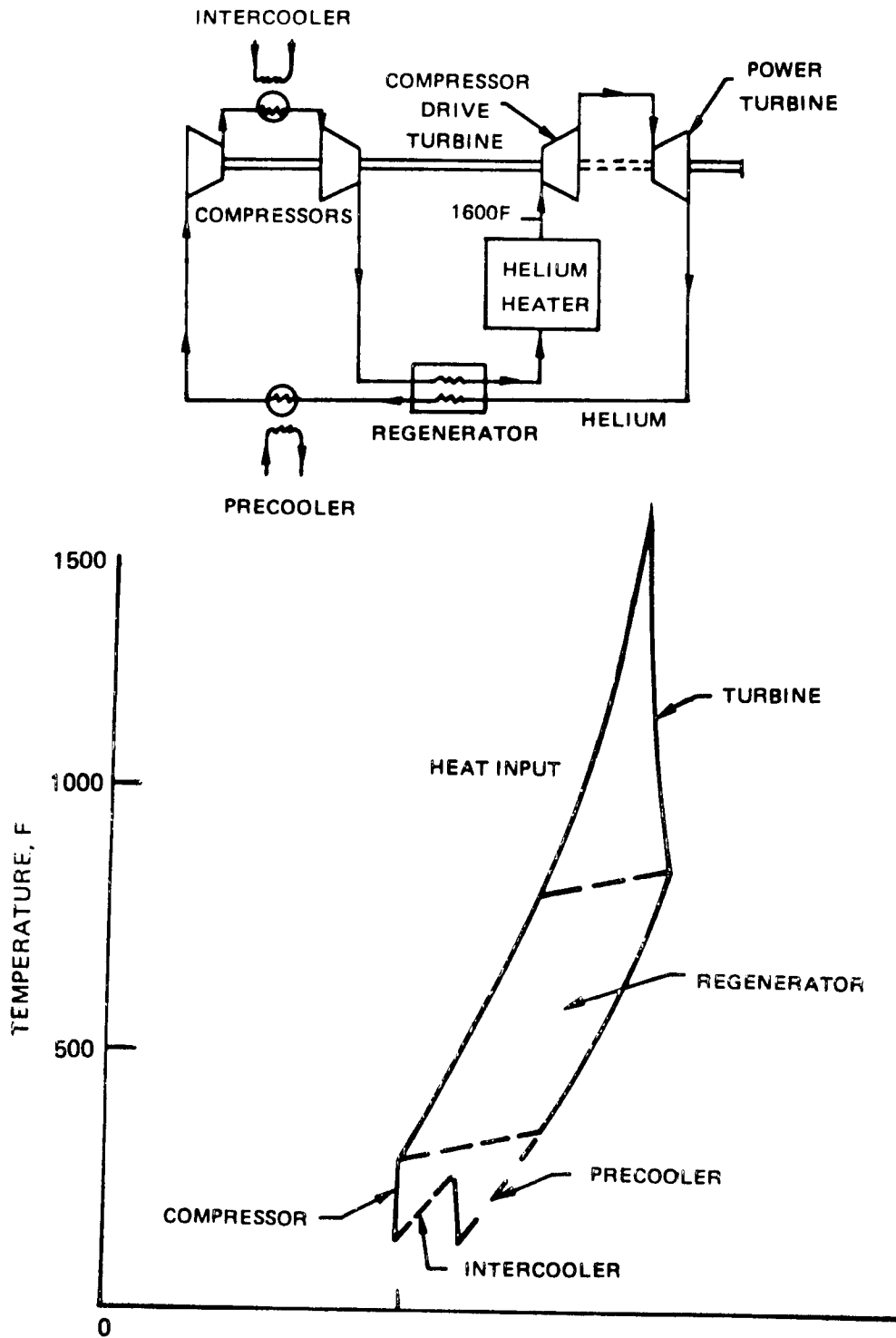
Figure 13 - Cycle diagram of the helium gas turbine system.

CLOSED–CYCLE HELIUM GAS TURBINE PERFORMANCE
1600°F TURBINE INLET

(1) SIMPLE CYCLE

(2) INTERCOOLING ONLY

(3) REGENERATION ONLY

(4) REGENERATION AND REHEAT

(5) INTERCOOLING AND REGENERATION

(6) INTERCOOLING, REGENERATION AND REHEAT
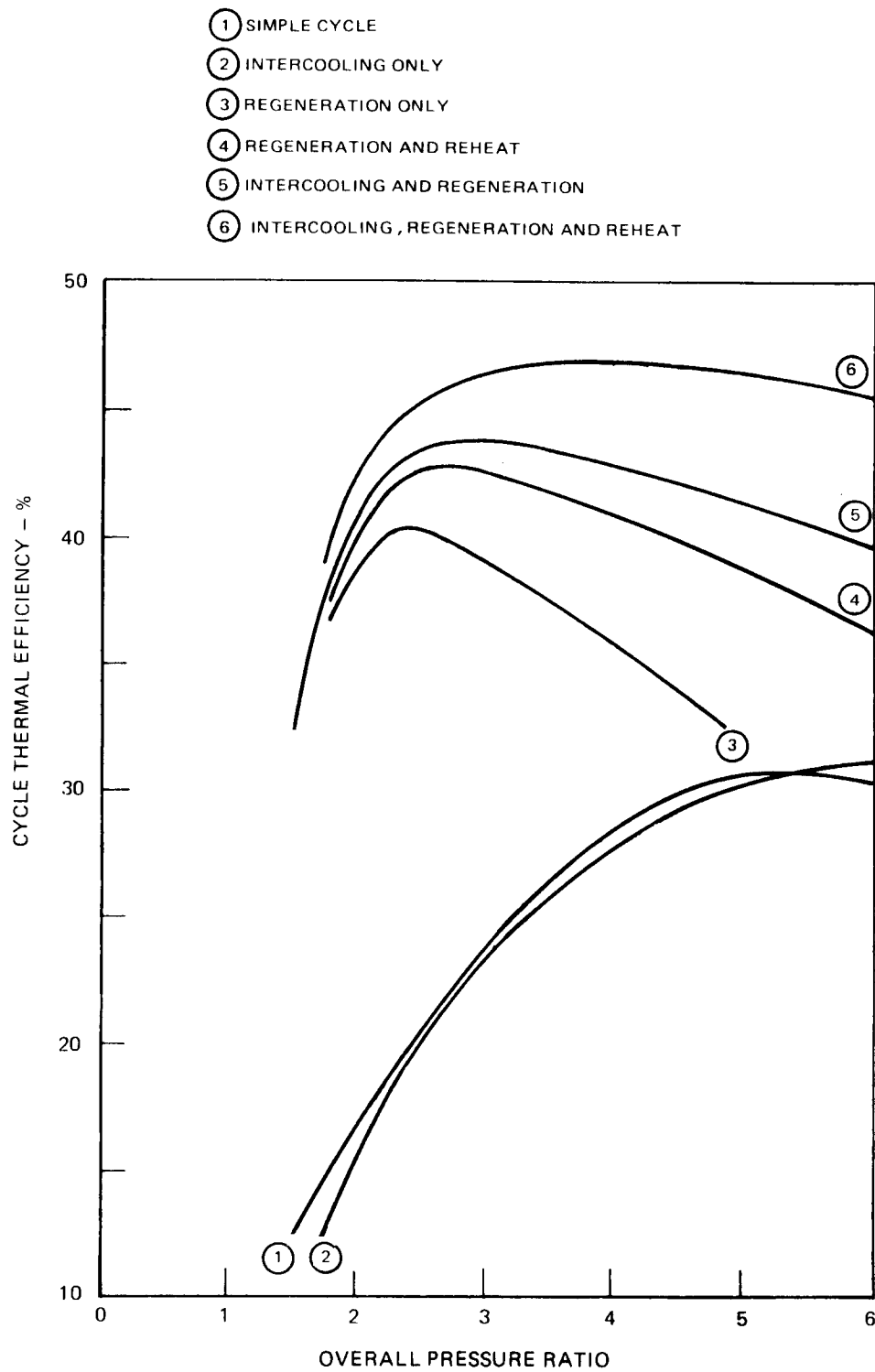
Figure 14 - Closed cycle helium gas turbine performance assuming 1600 F (871 C) turbine inlet temperature.

UWMAK–III POWER CONVERSION SYSTEM INTEGRATION SCHEMES
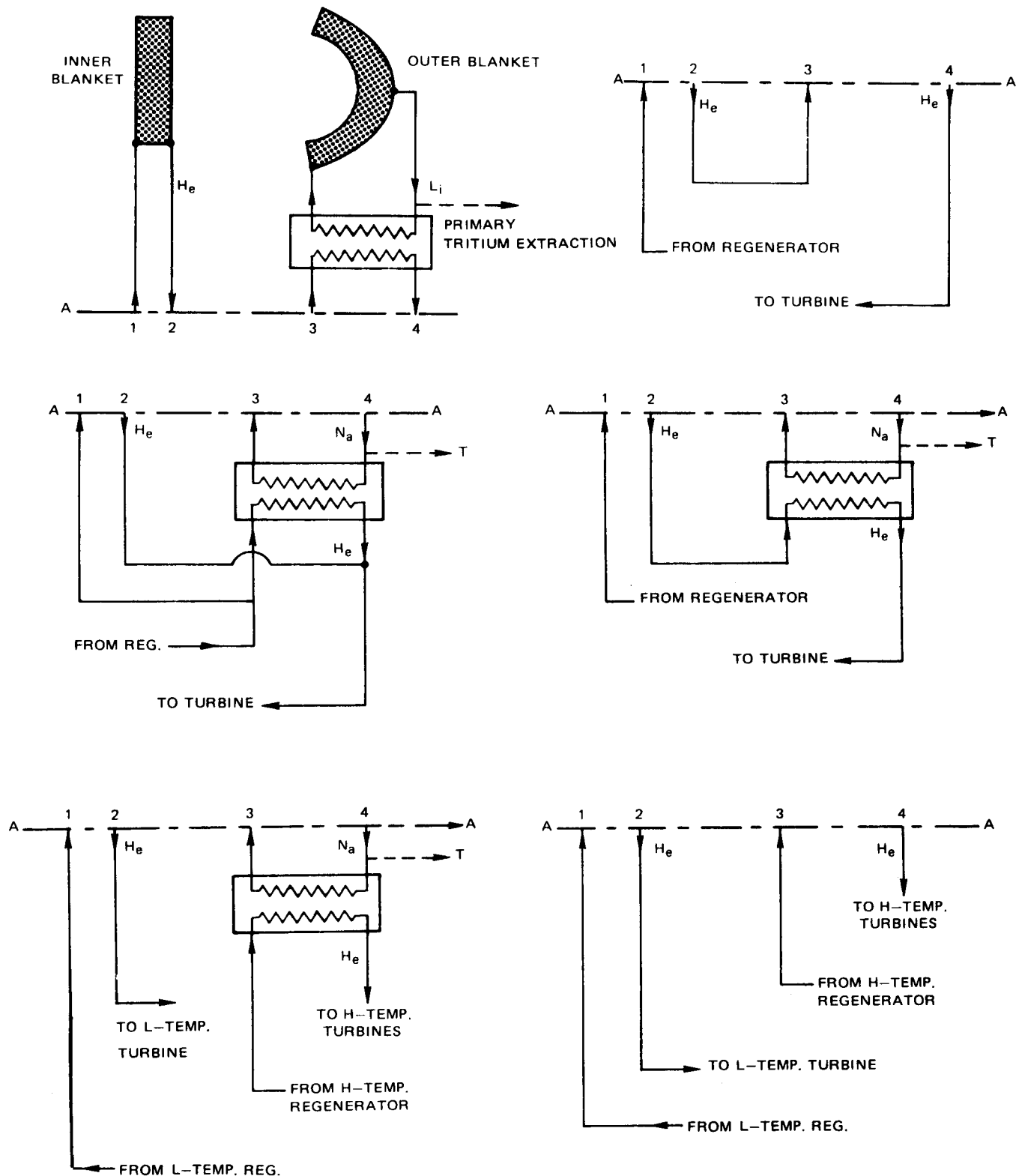
Figure 15 – Various integration schemes for the UWMAK-III power
conversion system.

REGENERATOR OUTLET TEMPERATURE RANGE

TURBINE INLET TEMPERATURE = 1600F
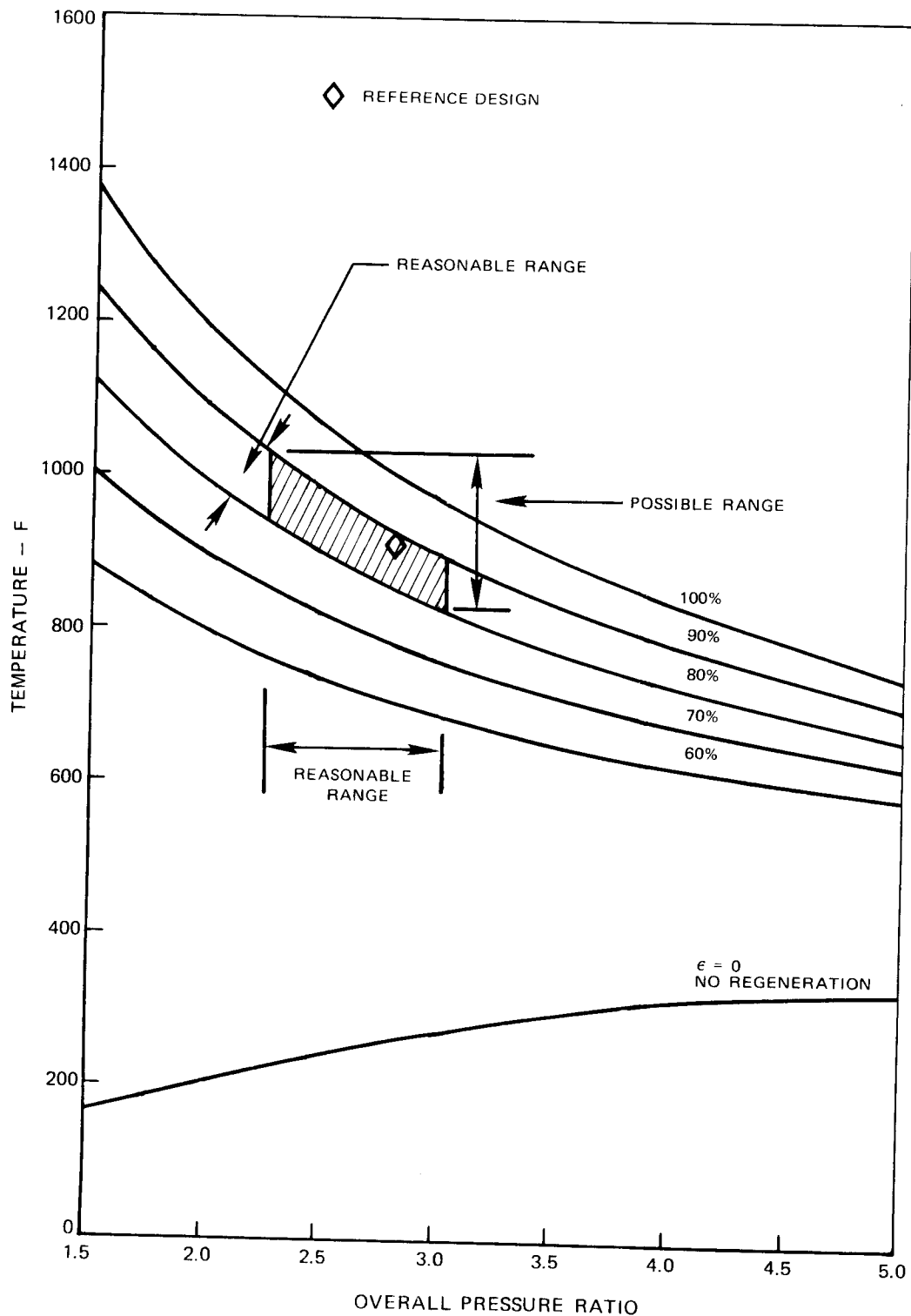
Figure 16 – The outlet range for the regenerator as a function of
the overall pressure ratio assuming the turbine inlet
temperature is 1600 F (871 C).

REFERENCE–

DESIGN CLOSED–CYCLE HELIUM GAS TURBINE SYSTEM FOR
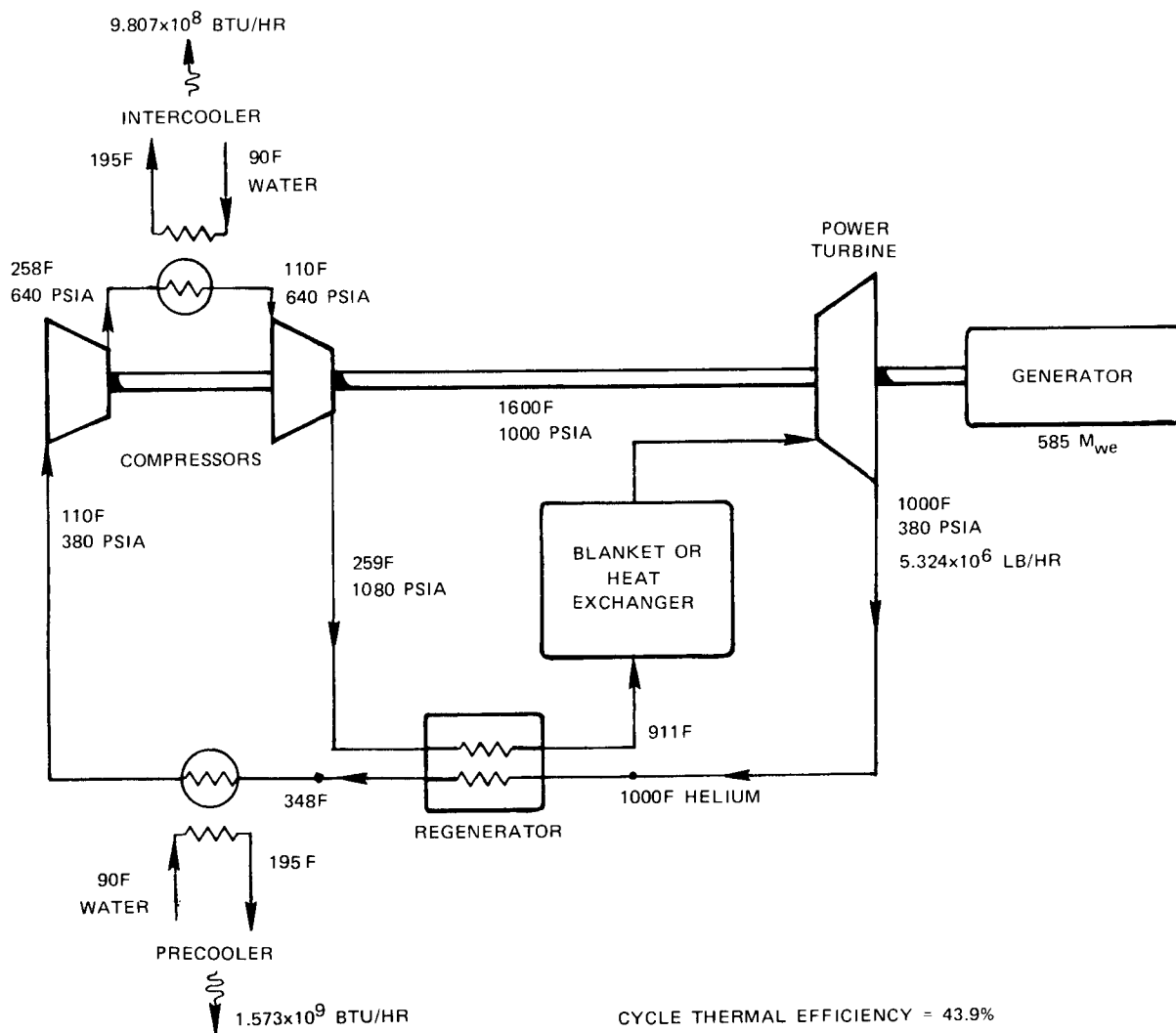
UWMAK–III FUSION PLANT

THREE LOOPS NEEDED

Figure 17 – Reference design of the closed cycle helium gas turbine
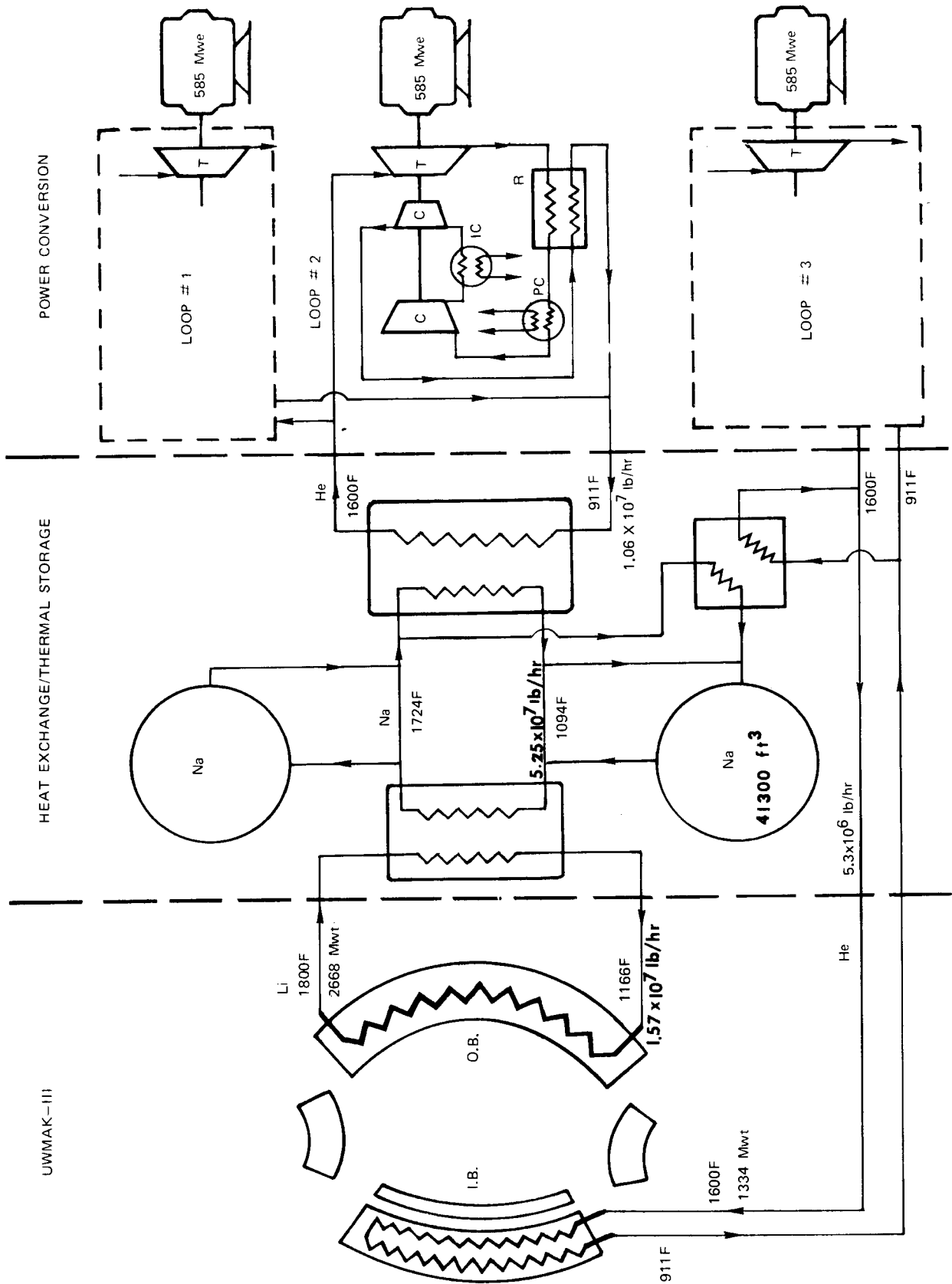system for UWMAK-III. Three identical loops would be
required.

Figure 18 – The final system arrangement and power flows for the UWMAK-III conceptual fusion power plant.

CLOSED-CYCLE HELIUM GAS TURBINES FOR UWMAK-III FUSION PLANT
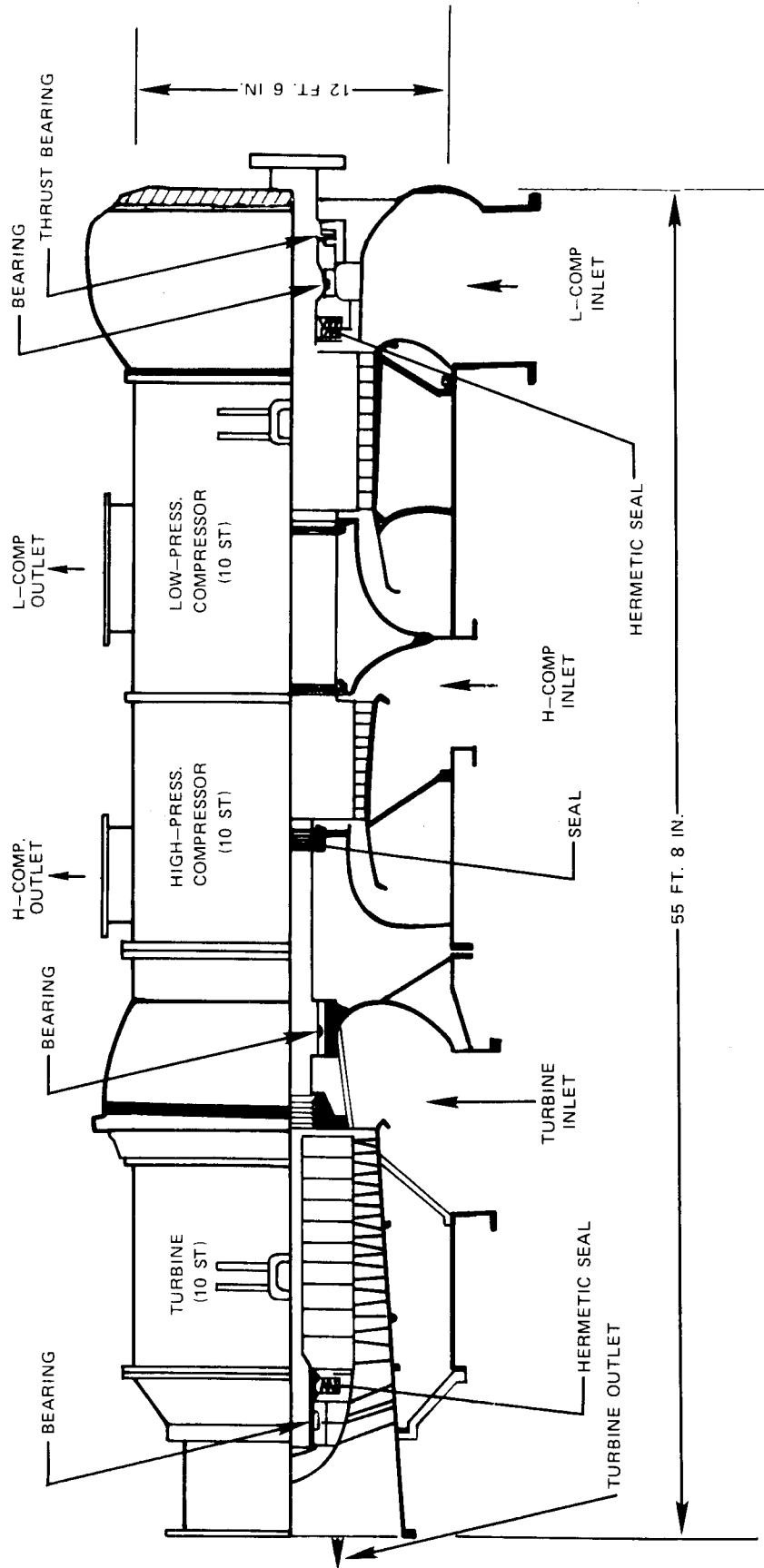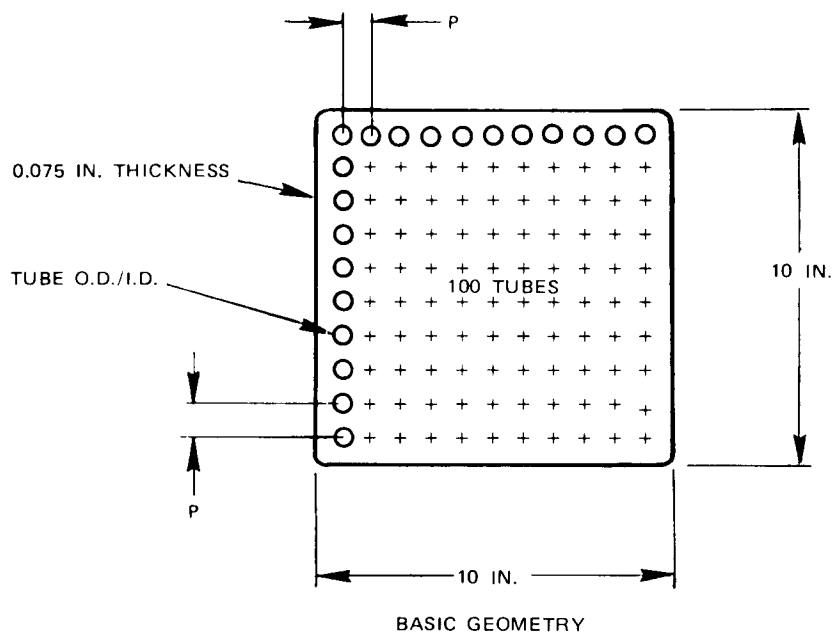
585 MWe UNIT OUTPUT, 3 NEEDED

Figure 19 - Conceptual design of the helium gas turbines.

HEAT EXCHANGER ELEMENTS FOR REGENERATOR, PRECOOLER AND INTERCOOLERS

BASIC GEOMETRY

	REGENERATOR	PRECOOLER AND INTERCOOLER
TUBE O.D./I.D., IN.	0.625/0.545	0.5/0.37
TUBE THICKNESS, IN.	0.04	0.065
PITCH, P, IN.	1.0	1.0
NO. OF TUBES PER ELEMENT	100	100
TUBE CIRCULAR PERIPHERY, FT OUTER/INNER	0.1636/0.1427	0.1309/0.0969
TOTAL CIRCULAR PERIPHERY, FT OUTER/INNER	16.36/14.27	13.09/9.69
TOTAL FLOW AREA, FT^2	0.00162	0.0007467
TOTAL TUBE FLOW AREA, FT^2	0.162	0.07467
EXTERNAL FLOW AREA, FT^2	0.4814	0.5581
RATIO OF OUTER/INNER FLOW AREA	2.97	7.47

Figure 20 – Characteristics of the heat exchanger elements for the regenerator, precooler and intercooler.

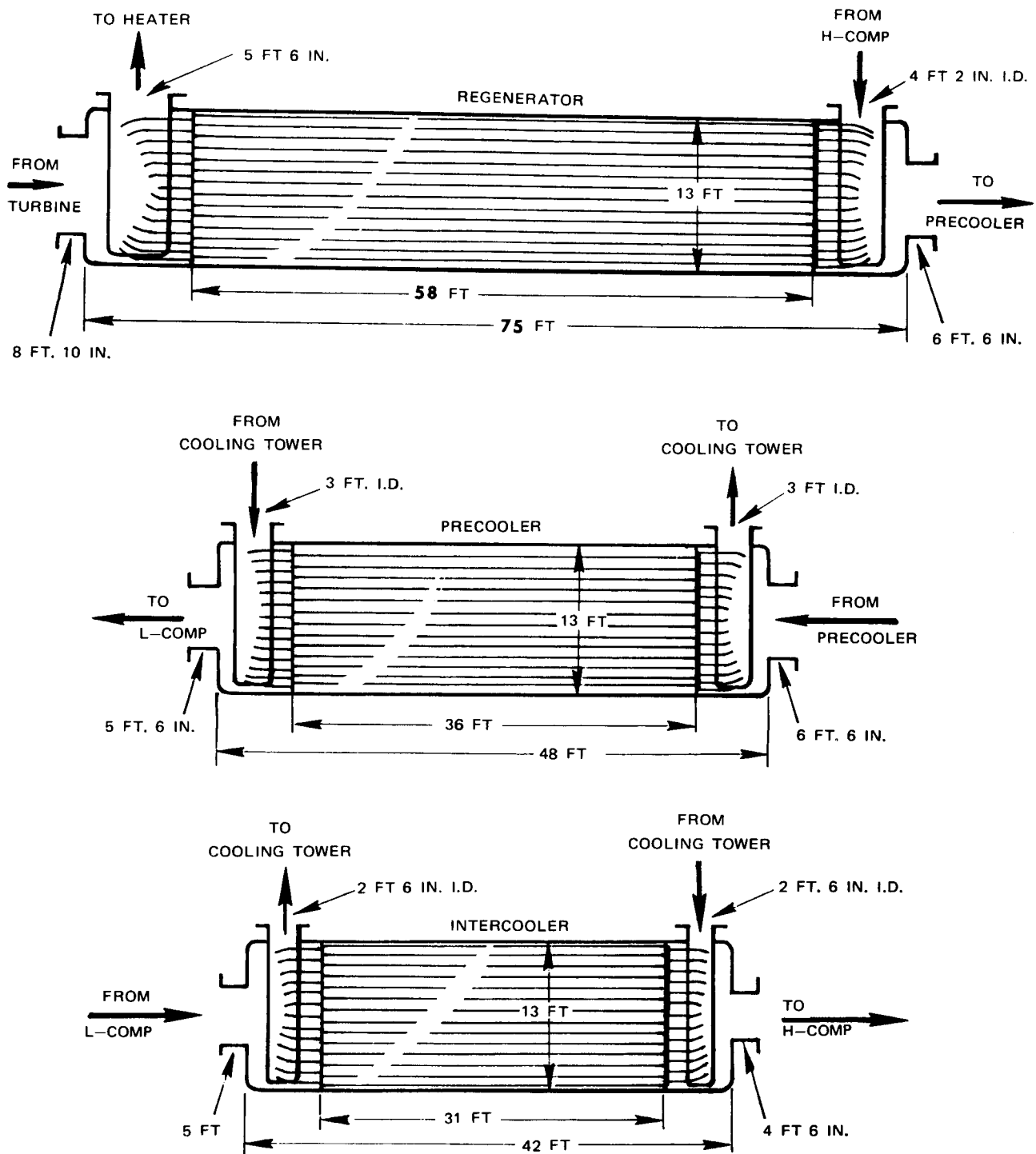# COMPARISON OF REGENERATOR, PRECOOLER AND INTERCOOLER SIZES

Figure 21 - Comparison of the sizes of the regenerator, precooler, and intercooler in the power cycle for UWMAK-III.

UWMAK-III FUSION POWERPLANT

1755 Mwe   40%efficiency

Reactor   Heat exchanger   Turbine generator   Thermal storage
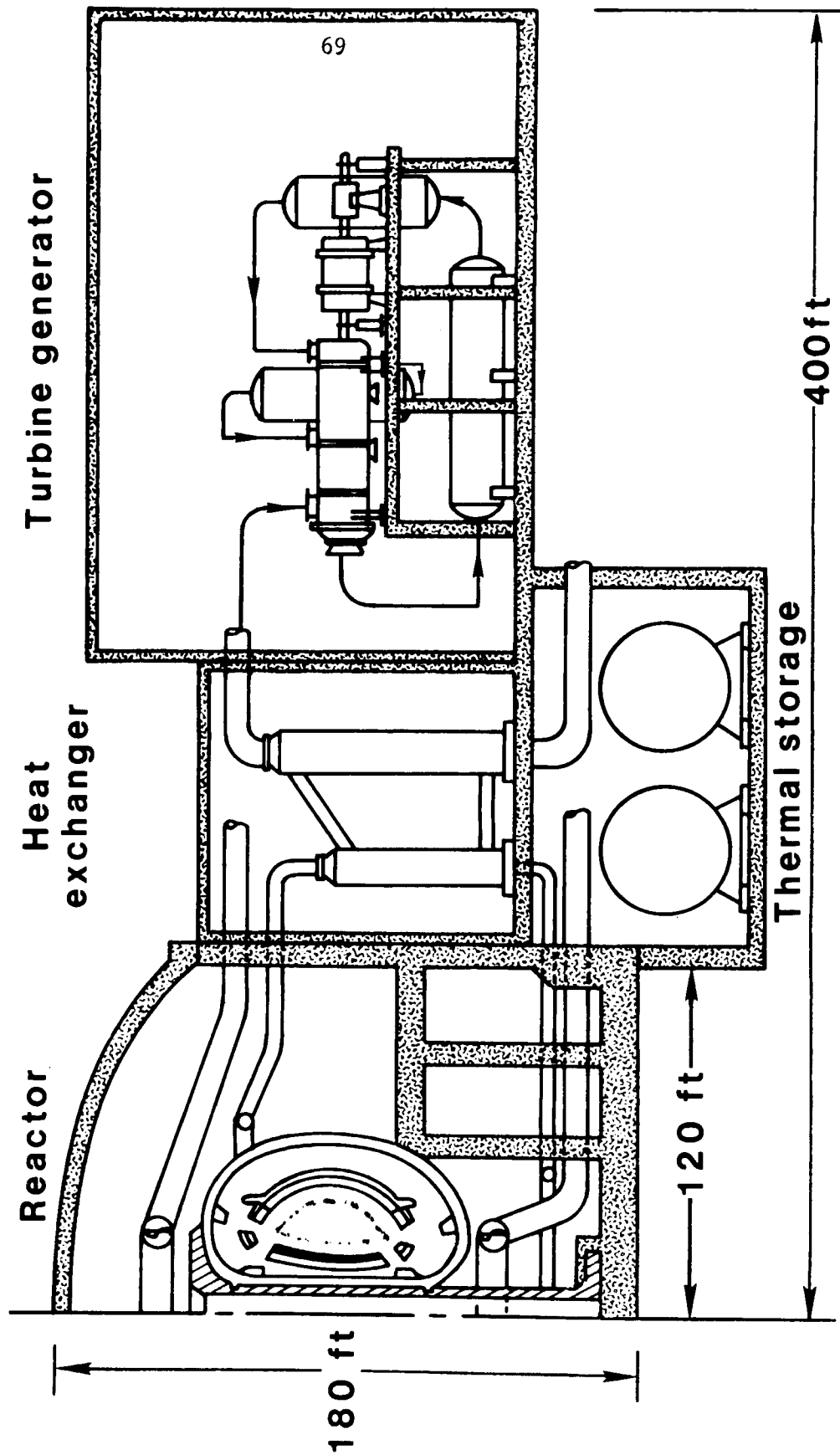
69

400 ft

120 ft

180 ft

Figure 22 – Relative locations and layout of the major power system components and the overall dimensions of the conceptual UWMAK-III fusion power system.